Bioorganic & Medicinal Chemistry 20 (2012) 2158–2171

Contents lists available at SciVerse ScienceDirect

Bioorganic & Medicinal Chemistry

journal homepage: www.elsevier.com/locate/bmc

Discovery of new orally effective analgesic and anti-inflammatory hybrid furoxanyl *N*-acylhydrazone derivatives

Paola Hernández [a], Mauricio Cabrera [a], María Laura Lavaggi [a], Laura Celano [b], Inés Tiscornia [c], Thiago Rodrigues da Costa [d], Leonor Thomson [b], Mariela Bollati-Fogolín [c], Ana Luisa P. Miranda [d], Lidia M. Lima [d], Eliezer J. Barreiro [d,*], Mercedes González [d,*], Hugo Cerecetto [d,*]

[a] *Grupo de Química Medicinal, Laboratorio de Química Orgánica, Facultad de Ciencias-Facultad de Química, Uruguay*
[b] *Laboratorio de Enzimología, Facultad de Ciencias, Universidad de la República, Montevideo, Uruguay*
[c] *Cell Biology Unit, Institut Pasteur de Montevideo, Uruguay*
[d] *LASSBio-Laboratório de Avaliação e Síntese de Substâncias Bioativas, Faculdade de Farmácia, Universidade Federal do Rio de Janeiro, Rio de Janeiro, Brazil*

ARTICLE INFO

Article history:
Received 6 November 2011
Revised 29 December 2011
Accepted 6 January 2012
Available online 2 February 2012

Keywords:
N-Acylhydrazone
Furoxane
Analgesic
Anti-inflammatory
Interleukin-8

ABSTRACT

We report the design, the synthesis and the biological evaluation of the analgesic and anti-inflammatory activities of furoxanyl *N*-acylhydrazones (furoxanyl-NAH) by applying molecular hybridization approach. Hybrid compounds with IL-8-release inhibition capabilities were identified. Among them, furoxanyl-NAH, **17**, and benzofuroxanyl-derivative, **24**, together with furoxanyl-NAH derivative, **31**, without IL-8 inhibition displayed both orally analgesic and anti-inflammatory activities. These hybrid derivatives do not have additional LOX- or COX-inhibition activities. For instance, LOX-inhibition by furoxanyl-NAH derivative, **42**, emerged as a structural lead to develop new inhibitors. The lack of mutagenicity of the active derivatives **17**, **31**, and **42**, allow us to propose them as candidates for further clinical studies. These results confirmed the success in the exploitation of hybridization strategy for identification of novel *N*-acylhydrazones (NAH) with optimized activities.

1. Introduction

Inflammation is defined as a complex defensive process, in which the body response to different injuries, characterized by the accumulation of local fluids and leukocytes with the objective of eliminating the noxious stimulus. In pathological conditions the evolution of persistent tissue damage by inflammatory cells is not suitably repaired.[1] An important group of inflammatory mediators are the eicosanoids which are able to activate and sensibilize nociceptors, leading to hyperalgesia.[2] Eicosanoids role in the genesis of several pathological states, for instance chronic inflammatory diseases, thrombosis and pain, is well established.[3,4] The non-steroidal anti-inflammatory drugs (NSAIDs) have been the most widely used drugs in the treatment of pain, that is, in rheumatoid arthritis, and in inflammatory diseases.

The majority of clinically employed NSAIDs are inhibitors of the prostaglandin synthase (cyclooxygenase, COX). The COX exists in two isoforms,[4] one (COX-1) with a cytoprotective role[5] and another (COX-2) with a role in the inflammation, pain, and fever.[6] Consequently, COX-2-inhibition appears as a therapeutic key for treatment of pain and inflammation. For example the COX-2 inhibitors celecoxib[7] and valdecoxib[8] (**1** and **2**, Scheme 1a) display anti-inflammatory activity. However cardiac toxicity, that is, with valdecoxib and rofecoxib (**3**, Scheme 1a),[9] has raised a cautionary flag on its research.[10] Though, COX-2 remains a very important pharmaceutical target for the treatment of debilitating diseases like rheumatoid arthritis and osteoarthritis and as a preventative agent for colon cancer. On the other hand, COX-2 inhibitors, like etoricoxib (**4**, Scheme 1a) used for the treatment of chronic rheumatoid and osteoarthritis, exhibit less gastrointestinal toxicity than traditional NSAIDs.[10] The gastrointestinal bleeding[11] and nephrotoxicity associated with NSAIDs long term use mandates the investigation of new analgesic and anti-inflammatory agents as a major challenge.[12–14]

Recently, we have described the *N*-acylhydrazone (NAH) subunit as the pharmacophoric framework of agents with potent antinociceptive,[15–17] antiplatelet,[18–20] anti-inflammatory,[21] and cardiac stimulant[22,23] activities. The relative acidity of the amide hydrogen of the NAH function, as well as its capacity for stabilizing free radicals give these compounds the ability of mimicking the bis-allylic moiety of unsaturated fatty acids and amides like, that is, arachidonic acid.[24,25] We have discovered the novel orally active

* Corresponding authors. Addresses: LASSBio—Laboratório de Avaliação e Síntese de Substâncias Bioativas, Faculdade de Farmácia, Universidade Federal do Rio de Janeiro, PO Box 68023, ZIP 21941902 Rio de Janeiro, RJ, Brazil. Tel./fax: +55 21 25626644 (E.J.B); Laboratorio de Química Orgánica, Facultad de Ciencias, Iguá 4225, 11400 Montevideo, Uruguay. Tel.: + 598 2 5258618x216; fax: +598 2 5250749 (M.G., H.C.).

E-mail addresses: ejbarreiro@ccsdecania.ufrj.br (E.J. Barreiro), megonzal@fq.edu.uy (M. González), hcerecet@fq.edu.uy (H. Cerecetto).

0968-0896/$ - see front matter © 2012 Elsevier Ltd. All rights reserved.
doi:10.1016/j.bmc.2012.01.034

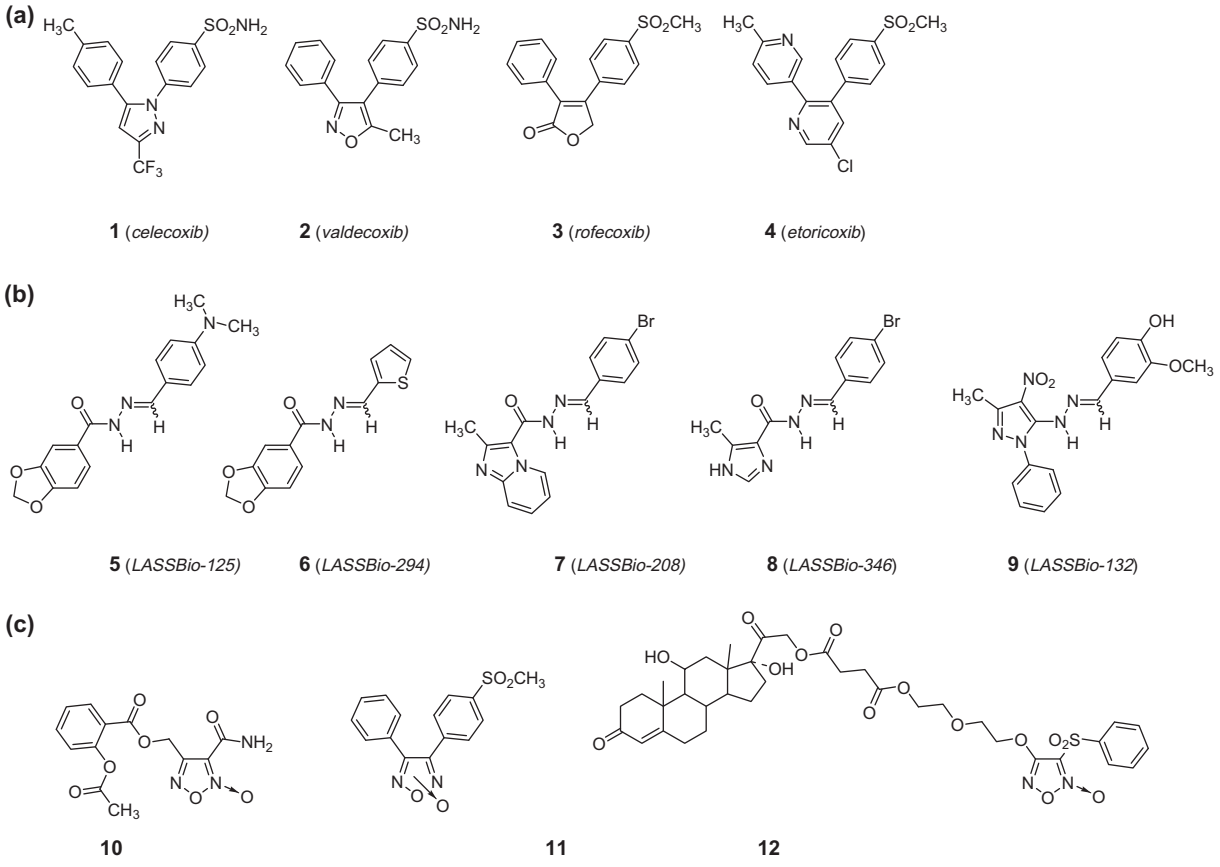

Scheme 1. (a) COX-2 inhibitors. (b) Orally active NAH derivatives previously developed. (c) Furoxans developed as analgesic and anti-inflammatory agents.

prototypes **5**–**7** (LASSBio-125, LASSBio-294, and LASSBio-208, respectively, Scheme 1b)[26,27] with analgesic profile, in the AcOH-induced mice model of abdominal constriction, and cardioactive effects in the case of derivative **6**.[22] Other interesting NAHs have been the derivatives belonging to the 2-methyl-imidazolyl-3-acylhydrazone class which were designed by applying molecular simplification on the imidazo[1,2-*a*]pyridine-derivative **7**. These NAH derivatives, that is, **8** (LASSBio-346, Scheme 1b), have important antinociceptive profiles[28] and anti-inflammatory activities.[29] Other interesting example, that belongs to hydrazone group, has been compound **9** (LASSBio-132, Scheme 1b).[30] This compound, designed as 5-lipoxygenase (LOX) inhibitor via its free-radical scavenger properties,[31] displayed in vivo anti-inflammatory activity with concomitant inhibition of neutrophil accumulation in the pleural cavity.

Recently, hybrid NSAID-furoxan derivatives, that is, **10** (Scheme 1c), have been developed as promising antiarthritic drugs.[32] These hybrid compounds, designed as COX inhibitors without gastrotoxic effects due to its potential nitric oxide (NO) release capability, have demonstrated ability to inhibit tumor necrosis factor-alpha (TNFα) release from both monocytes and macrophages. Interestingly, furoxan (1,2,5-oxadiazole N-oxide, Fx) system has also exhibited bioisosterism with the 2-(5*H*)furanone moiety,[33] present in COX-2-inhibitor rofecoxib. The mixture of N-oxide **11** (Scheme 1c) is the most selective COX-2/COX-1 developed Fx. The successful use of the Fx moiety in the generation of hybrid glucocorticoid has also been described (compound **12**, Scheme 1c).[34] Apart from the gastroprotective activity, the Fx pharmacophore is able to act as regulator of expression- and activity- of COX and -LOX, by NO-arachidonic acid release-modulation,[35,36] or as a free-radical scavenger moiety[37] modifying the intracellular redox-balance.

These approaches encourage us to design and develop hybrid agents, which combine NAH and Fx moieties, with potential analgesic and anti-inflammatory properties. In the design stage we reckoned the COX-2-inhibitors valdecoxib and etoricoxib (**2** and **4**, respectively, Scheme 1a) as chemical templates for the development of new compounds combining in these structures molecular moieties from NAH-parent compounds **5–9** and 3-methyl-4-furoxanyl, 4-phenyl-3-furoxanyl or 5-benzofuroxanyl as NO-release and/or free radical-scavenger moieties (Scheme 2). In our planning the acyl moiety of NAH (R_1) was pyridine-3-yl (like **4**), benzo[*d*][1,3]dioxole-5-yl (like **5** and **6**), 4*H*-imidazo[1,2-*a*]pyridine-3-yl (like **7**), 1*H*-imidazole-4-yl (like **8**), 1-phenyl-1*H*-pyrazole-4-yl (like **9**), furoxan-3- or -4-yl (as potential bioisoster of 5-methylisoxazole-4-yl present in compound **2**). On the other hand, the hydrazonyl moiety of NAH (R_2) was 4-(dimethylamino)phenyl (like **5**), 2-thienyl (like **6**), 4-bromophenyl (like **7** and **8**), 4-hydroxy-3-methoxyphenyl (like **9**), or the furoxanyl moieties. Additionally, in this position other substituents were investigated, that is, 2-furyl, 5-nitro-2-thienyl, 5-nitro-2-furyl, 3-hydroxy-4-methoxyphenyl, 3,4-dimethoxyphenyl, benzo[*d*][1,3]dioxole-5-yl, 2-hydroxyphenyl, and 4-carboxyphenyl.

Thirty two hybrid furoxanyl *N*-acylhydrazones (furoxanyl-NAH) have been synthesized and their in vitro abilities to decrease the release of the proinflammatory cytokine interleukin-8 (IL-8, CXCL8 according to the new nomenclature)[38] in HT-29-NF-κB-hrGFP cells have been determined. The best IL-8-release inhibitors with the lowest in vitro cytotoxicity in J774 murine macrophages were used orally to determine analgesic and anti-inflammatory properties in mice. Besides, the anti-inflammatory mechanisms by which the compounds act will be discussed. In this sense we studied inhibitory properties on COX-1, COX-2, LOX, and NO-releasing capability.

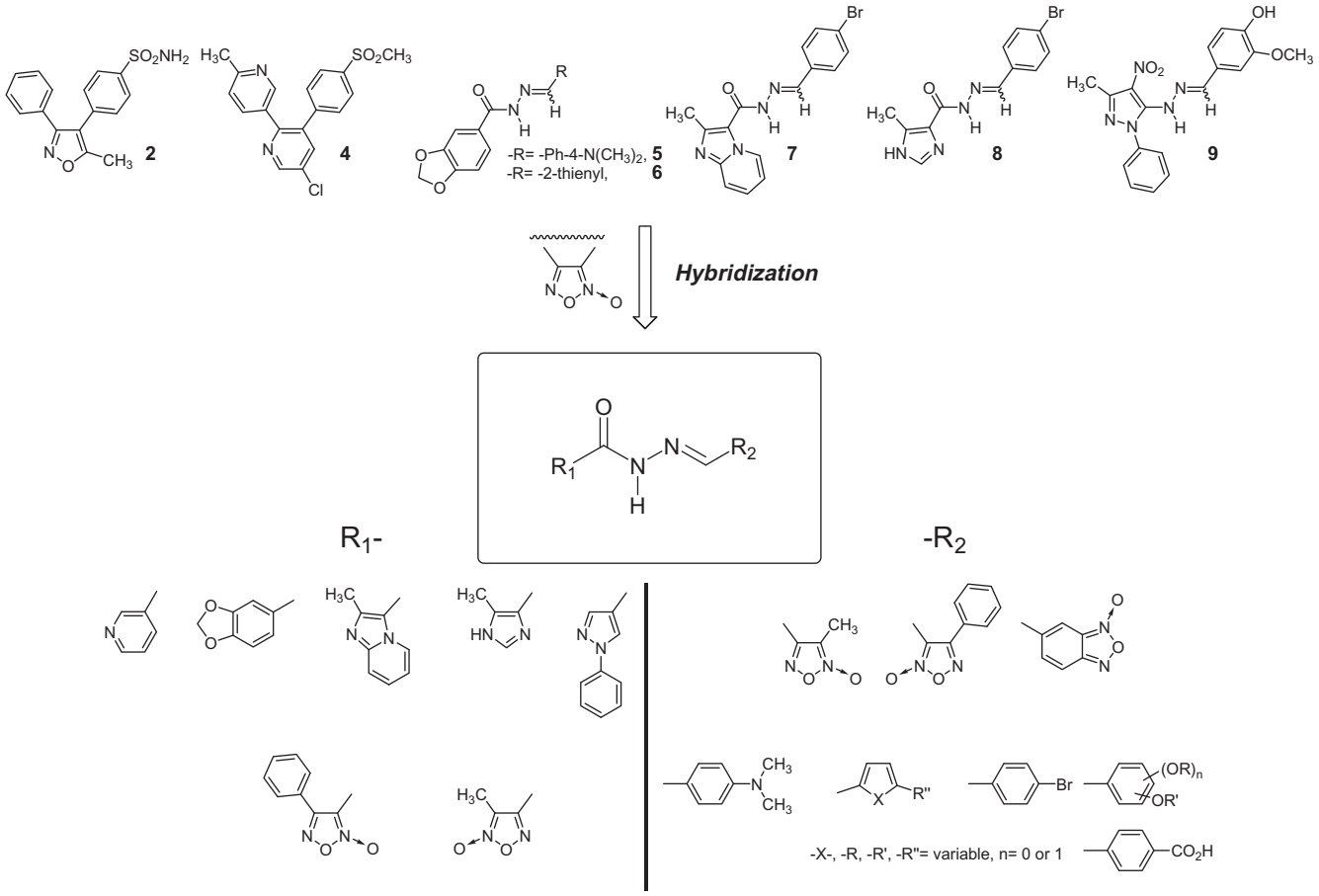

Scheme 2. Design of new hybrid-NAH as potential analgesic and anti-inflammatory agents.

Moreover, the most promising derivatives were studied for their mutagenicities in order to confirm their potentials as candidate drugs.

2. Methods and results

2.1. Chemistry

The first compounds synthesized, where R_2 were the furoxanyl moieties, were the 3-pyridinyl derivatives **13–15** (Scheme 3a) furoxanyl-hybrid of parent compound etoricoxib (**4**, Scheme 1). Nicotinic acid was used as starting material followed by the preparation of the corresponding hydrazide[39,40] and finally the condensation with furoxanyl aldehydes ((**I**), (**II**) or (**III**)). The same procedure was used to prepare the hybrid products **16–27** (Scheme 3a) using the hydrazides[27,28,40–43] derived from benzo[*d*][1,3]dioxole, 4*H*-imidazo[1,2-*a*]pyridine, 1*H*-imidazole, and 1-phenyl-1*H*-pyrazole where the parent compounds are the NAH **5–9** (Scheme 1). When R_1 was a furoxanyl moiety, derivatives **28–43** were prepared according to shown in Scheme 3b. The common reagent, hydrazide (**IV**), was prepared via the transformation of the aldehyde (**I**) to the corresponding methyl ester[42] by treatment with manganese dioxide and potassium cyanide in methanol followed by the reaction with 0.9 equiv of hydrazine hydrate. The following condensation with different aldehydes produced derivatives **28–43** in good yields. The high reactivity of aldehyde (**II**) (3-formyl-4-phenylfuroxan) did not allow us to generate hydrazide (**VI**) using the same procedure employed for preparation of (**IV**) (i. MeOH/KCN/MnO_2; ii. NH_2NH_2), consequently we used the acid (**V**) as the starting material and, by activation with CDI,[44] we generated the desired intermediate (**VI**) in excellent yield (Scheme 3b). Derivative **44** was prepared using this intermediate. All the compounds were characterized by ^{1}H NMR, ^{13}C NMR, IR and MS. Except for derivatives **13** and **25** (see example in Supplementary data) and according to the NMR experiments, ^{1}H NMR[45] and NOE-diff (see examples in Supplementary data), and characteristic fragmentations in MS experiments (see example in Supplementary data the NAH were obtained as the *E*-isomers around the ylidenic moiety. In the case of compounds **13** and **25** the main stereoisomers were the *E*, with ratio of *E:Z* 95:5 and 67:33, respectively. The purity was established by TLC and microanalysis. Only compounds with analytical results for C, H and N, within ± 0.4 of the theoretical values were considered pure enough.

2.2. Biological characterization

2.2.1. In vitro evaluation of NF-κB pathway inhibition and level of IL-8

The in vitro ability to decrease activation of NF-κB and the level of IL-8 was evaluated using a human pathway-specific reporter cell system (HT-29-NF-κB-hrGFP). Human intestinal epithelial cells HT-29 stably transfected with pNF-κB-hrGFP plasmid were stimulated with the pro-inflammatory cytokine TNF-α. The activation of NF-κB was estimated by measuring the percentage of GFP-expressing cells while the IL-8-secretion was quantified in the supernatant by flow cytometry (see example in Supplementary data). Both determinations were performed in the absence and presence of hybrid-NAH (Table 1). The compounds were evaluated at the highest non-cytotoxic doses (100% of cell survival on HT-29-NF-κB-hrGFP cells). Thalidomide (Thal, Table 1) was used as reference drug.

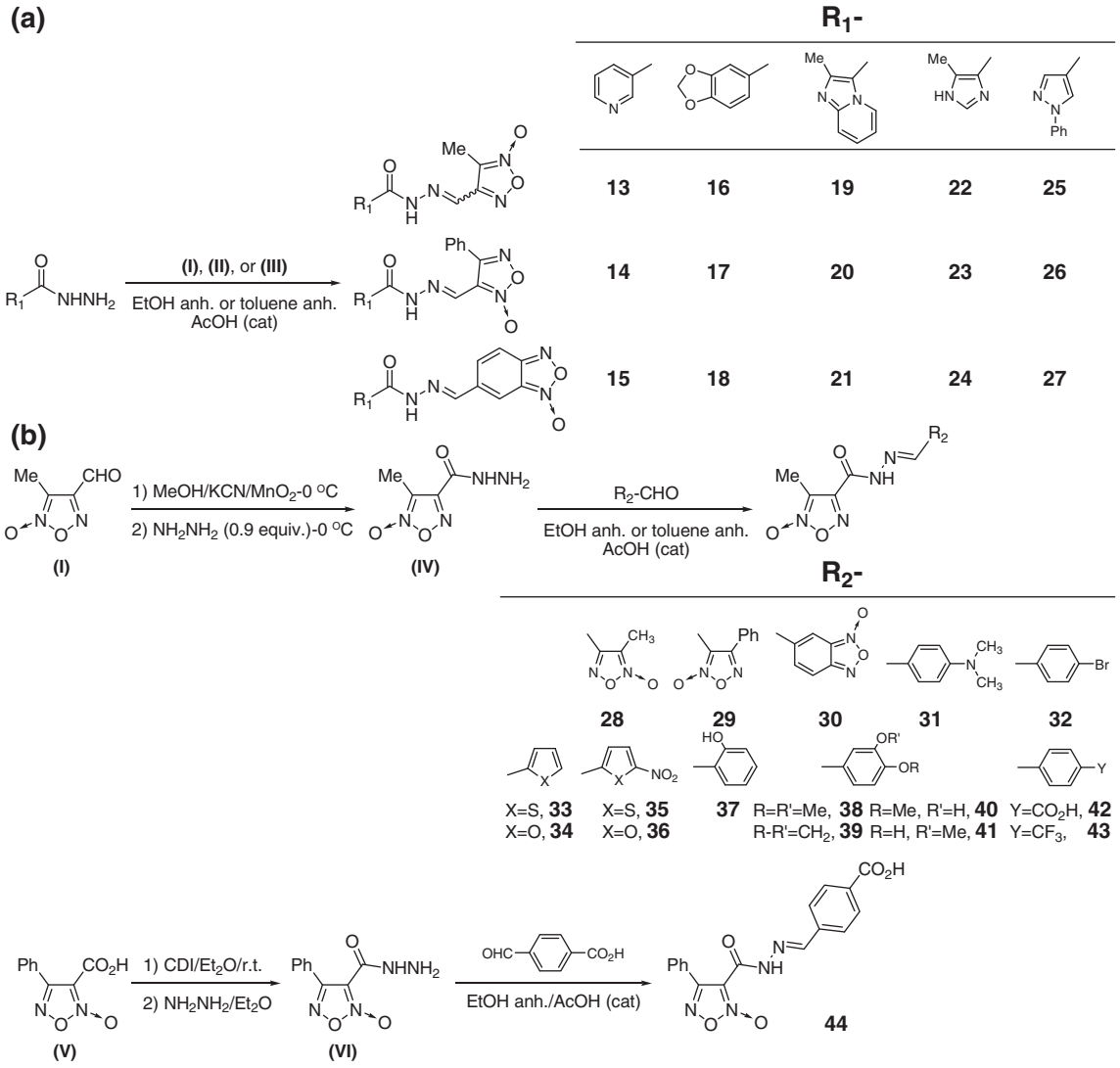

Scheme 3. Synthetic procedures used to prepare the new derivatives. (I): 3-methyl-4-formylfuroxan; (II): 3-formyl-4-phenylfuroxan; (III): 5-formylbenzofuroxan.

Additionally, two hydrazides, benzo[*d*][1,3]dioxole-5-carbohydrazide and 2-methyl-4*H*-imidazo[1,2-*a*]pyridine-3-carbohydrazide, **45** and **46** (Table 1), respectively, and the well-known NO-releasing compound, 3,4-bis(phenylsulfonyl)furoxan (**47**, Table 1), were included in order to evaluate the effect of reducing IL-8 levels. Concomitantly, the cytotoxicity against murine cells, J774 macrophages, was evaluated in order to select the best compounds to progress to in vivo studies (Table 1). Controls of NAH without TNF-α stimulation were also included with the aim to evaluate the potential pro-inflammatory activity of the compounds, finding that hybrid-NAHs were not pro-inflammatories per se. Most of the hybrid-NAH displayed the same profile in both biological systems (see Supplementary data). Hybrid-NAH **15, 17, 18, 20, 24** inhibited releasing IL-8 and activation of NF-κB in the same order. But others affected more the release of IL-8 as Thal do, that is, **28**–**33**, **36**, **38**, **40**–**42**. The hybrid-NAH **17**, derived from furoxan, was the best in vitro IL-8 releasing inhibitor being 16 times more potent than Thal at the same dose (400 μM). The hybrid NAHs benzofuroxan **15** and furoxan **20** also showed better ability to inhibit IL-8 production than Thal while benzofuroxan **24** and furoxans **28**, **30**, **32**, **33**, **36**, **38**, **40**, and **42** were as active as Thal. On the other hand, NAH **23** was an IL-8 release promotor, at an intermedium dose (200 μM), duplicating this parameter respect to untreated cells.

2.2.2. In vivo evaluation of analgesia and anti-inflammation

Hybrid-NAHs, **15**, **17**, **20**, **24**, **28**, **31**–**33**, **36**, **38**, and **42**, were selected for further pharmacological evaluation on pain models and temporal and chronic inflammation models in order to confirm its potential as drug candidates. The evaluation of the analgesic profile of NAH derivatives was performed using the classical acetic acid-induced mice abdominal constrictions assay,[26] administering orally at 100 μmol/kg and using dipyrone and indomethacin (Ind) as standard drugs (Table 2). The hybrid NAHs derived from benzofuroxan **15** and **24**, and derived from furoxan **17** were the best inhibitors of abdominal constrictions having values in the order of the reference drug. The hybrid-NAHs derived from methylfuroxan displayed lower inhibition capabilities. Derivatives **31** and **32** exhibited better inhibition at 60 min (Table 2) compared to other compounds. For compounds **15**, **17**, **24**, and **31** we performed a modified version of the classical hot-plate method,[26] suitable for measuring inflammatory nociception (hyperalgesia) through the previous treatment of the animals with carrageenan (Fig. 1).

In spite of the poor efficacy, furoxanyl-NAHs **17** and **24** reduced in ca. 14% the Δ latency time in comparison with the vehicle group, at 1 h for **17** and 3 h for **24**. Thus indicate their ability to control the hyperalgesic stimuli in inflammatory pain models. These data were in agreement with the in vitro results where the reduction of IL-8

Table 1
NF-kB pathway inhibition capabilities, IL-8 levels and J774 cytotoxicities of new hybrid-NAHs

Compd	Doses (μM)	%GFP[a]	%IL-8[b]	$IC_{50,J774}$[c] (μM)	Compd	Doses (μM)	%GFP[a]	%IL-8[b]	$IC_{50,J774}$[c] (μM)
13	100	112 ± 2	105 ± 4	>400	**28**	100	127 ± 4	65 ± 20	>400
14	25	114 ± 6	138 ± 3	195 ± 2	**29**	100	122 ± 2	77 ± 1	>400
15	50	66 ± 10	29 ± 2	31 ± 1	**30**	400	121 ± 5	68 ± 21	>400
16	400	102 ± 1	106 ± 16	132 ± 1	**31**	100	150 ± 1	98 ± 3	129 ± 1
17	100	12 ± 1	4 ± 1	191 ± 2	**32**	100	126 ± 4	61 ± 6	162 ± 2
18	400	87 ± 16	64 ± 5	141 ± 2	**33**	100	122 ± 2	75 ± 10	>400
19	400	120 ± 4	77 ± 23	>400	**34**	100	99 ± 14	82 ± 19	>400
20	400	32 ± 9	38 ± 6	56 ± 1	**35**	100	111 ± 4	—[d]	68 ± 1
21	400	104 ± 1	76 ± 6	>400	**36**	100	136 ± 2	48 ± 1	96 ± 1
22	100	126 ± 3	103 ± 16	>400	**37**	100	55 ± 1	—	246 ± 2
23	200	103 ± 3	199 ± 1	>400	**38**	400	120 ± 1	68 ± 10	>400
24	50	71 ± 6	51 ± 1	38 ± 1	**39**	100	97 ± 8	98 ± 3	>400
25	100	80 ± 21	—	295 ± 3	**40**	400	117 ± 1	59 ± 30	>400
26	400	105 ± 6	—	42 ± 1	**41**	100	149 ± 9	77 ± 2	>400
27	—	—	—	37 ± 1	**42**	400	125 ± 2	53 ± 2	>400
					43	400	55 ± 1	—	>400
					44	50	115 ± 1	114 ± 31	>300
Thal[e]	400	116 ± 6	57 ± 5	>400	**45**[f]	50	118 ± 1	—	>400
	200	114 ± 3	77 ± 4		**46**[g]	50	111 ± 1	—	>400
	100	126 ± 13	63 ± 13		**47**[h]	20	6 ± 1	6 ± 5	—

[a] %GFP: percentage of GFP—expressing cells normalized against the TNF-α control cells treated with DMSO ⩽0.5% (±SD).
[b] %IL-8: percentage of IL-8 production respect to TNF-α control cells treated with DMSO ⩽0.5% (±SD).
[c] $IC_{50,J774}$: IC_{50} against murine macrophages J774.
[d] —: not determined.
[e] Thal: thalidomide.
[f] Benzo[*d*][1,3]dioxole-5-carbohydrazide.
[g] 2-Methyl-4*H*-imidazo[1,2-*a*]pyridine-3-carbohydrazide.
[h] 3,4-Bis(phenylsulfonyl)furoxan. Thal, and compounds **45**–**47** were included as controls.

Table 2
Analgesic and anti-inflammatory profiles of new selected NAHs and controls in AcOH-induced abdominal constriction test in mice and carrageenan-induced rat paw edema assay

Compd	Constrictions inhibition at 30 min[a] (%)	Constrictions inhibition at 60 min (%)	δ Paw volume (edema inhibition[c] (%)
15	35 ± 9*	—[b]	0
17	42 ± 8*	—	0
20	2 ± 5	14 ± 5	18 ± 5
24	46 ± 13**	—	31 ± 9**
28	—	14 ± 6	10 ± 4
31	—	22 ± 5	19 ± 7*
32	—	23 ± 6	0
33	—	14 ± 4	0
36	—	13 ± 5	14 ± 3
38	—	17 ± 6	4 ± 1
42	—	0	16 ± 8
Ind[d]	—	44 ± 8**	61 ± 4**
Dipyrone	36*,[e]	—	—
Nimesulide[f]	—	—	57.5**,[g]
6[f]	—	—	30 ± 3**,[g]

[a] % of inhibition obtained by comparison with vehicle control group.
[b] —: not determined.
[c] Respect to untreated controls (100%). The results refer to the 3rd hour.
[d] Ind: Indomethacin.
[e] From Ref. 26
[f] Evaluated at 300 μmol/kg.
[g] From Ref. 21 *p <0.05, **p <0.01. Student t-test.

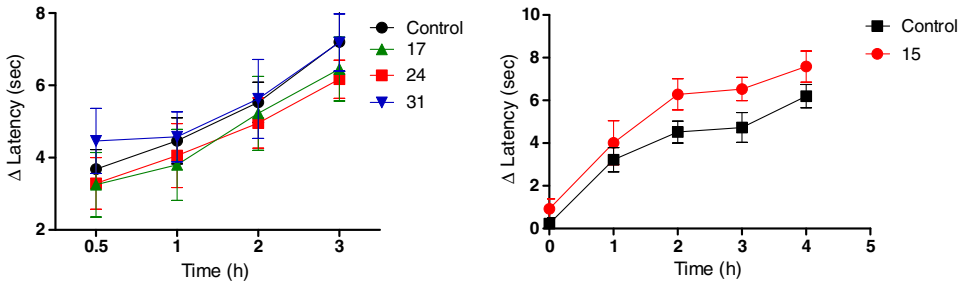

Figure 1. Effect of NAHs **15**, **17**, **24**, and **31** against carrageen-induced hyperalgesia in rats, at 100 μmol/kg, po. Each point represents the mean ± SEM of 8–10 experimental values. Controls correspond to treatment with vehicle.

conduces to the reduction of the hyperalgesic response.[46] On the other hand, hybrid benzofuroxan **15** and methylfuroxan **31** were unable to reduce inflammatory nociception. The furoxanyl-NAH **15** was active in vitro in the IL-8-model however it was inactive in this in vivo assay. Probably, it could be the result of the low bioavailability of derivative **15** in the inflammation site.

For the in vivo pharmacological evaluation of furoxanyl-NAHs anti-inflammatory activities, the carrageenan induced rat paw edema model, a classic model of acute inflammation,[21] was used. Ind, at 100 μmol/kg, and nimesulide, a diarylether anti-inflammatory drug and the NAH-parent compound **6** were used, at 300 μmol/kg, as controls. All compounds were administered orally (100 μmol/kg) 1 h before inflammatory challenge. The paws volumes were measured, for all the NAHs, 3 h after the subplantar injection (Table 2) and temporally for **15**, **17**, and **31** (Fig. 2). The edema was calculated as the volume variation between the carrageenan and saline treated paw. Between the analyzed hybrid-NAHs the benzofuroxan **24** and the furoxan **31** were as effective on rat paw edema prevention as the NAH-parent compound **6** (evaluated at 300 μmol/kg). Furoxanyl-NAH **15** and **17**, the major in vitro IL-8 inhibitors, are poor or unable to diminishing the edema at the 1st and 2nd hours (**15** produce only ca. 12%, Fig. 2). Contrarily furoxan **31**, a slightly in vitro IL-8 inhibitor, showed good ability to reduce edema since the 1st hour of study, ca. 23%, achieving a 25% of protection at the 4th hour of the study (Fig. 2). For the complete in vivo studied NAHs population no clear correlation between in vitro IL-8 inhibition and in vivo edema diminution was observed. However, the methylfuroxan series, NAHs **28**, **31–33**, **36**, **38**, and **42**, show certain tendency in the correlation. In this relationship compound **31** could be considered as an outlier suggesting a different mechanism of action (see Supplementary data).

2.3. Studying the mechanism of analgesia and anti-inflammation

The in vivo anti-inflammatory properties of furoxanyl-NAH **24** could be explained by its in vitro inhibitory action on IL-8 release. But for some of the rest NAH the in vivo analgesia and anti-inflammation displayed activities are not clearly related, so more studies were done to access to the biological targets. Consequently, LOX-, COX-1-, and COX-2-inhibition and capability to produce NO were studied.

A commercial kit of soybean lipoxygenase-15[47] was used to determine the inhibitory effect of selected NAH in the lipooxygenation process promoted by hydrogen peroxide. Quercetin (Quer), at 4 μM, was employed as positive control (Table 3). In the case of NAH **28** the LOX-inhibition capabilities could be indicating that this mechanism is the responsible of the in vivo analgesia (Table 2).

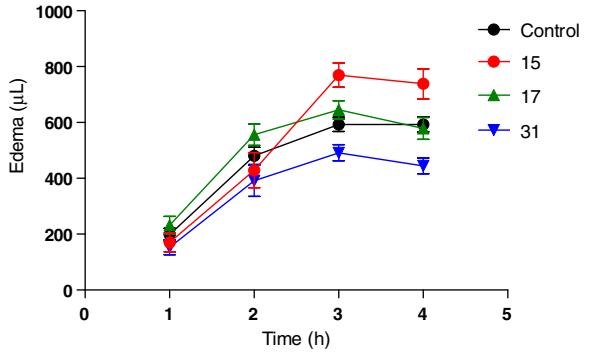

Figure 2. Time course effect of NAHs on carrageenan induced rat paw edema. Results are expressed in terms of mean ± SEM (n = 8–10 animals per group). Control corresponds to treatment with vehicle.

However in the case of NAH **31** its remarkable in vivo activities were not related to LOX-inhibition. In general, the methylfuroxan derivatives were better LOX-inhibitors than the corresponding phenylfuroxan- or benzofuroxan-analogues (i.e., compare inhibition capabilities between 3-pyridinyl derivatives **13**, **14**, and **15** or 3-imidazolyl derivatives **22**, and **24**). In the series of methylfuroxan-NAHs, **28–44**, the better LOX-inhibitors were **28**, **37**, **40**, **42**, and **43**, being the acid **42** the best one. The phenyl-analogue **44** also displayed good LOX-inhibition capability at the assayed dose. Interestingly, the best in vitro LOX-inhibitor and a good NF-κB pathway inhibitor (Table 1), NAH **42**, did not produce in vivo analgesia or anti-inflammatory activity (Table 2) probably as result of poor bioavailability.

NAHs **17**, **24**, and **31** were characterized for their COX-1 and COX-2 inhibitory activity using a COX inhibitor screening assay kit. Ind was employed as positive control (Table 4).[48] Comparing to Ind the analyzed NAH were poor COXs inhibitors and their biological in vivo activities seem to be not related with these inhibitions. The NAHs were better COX-1- than COX-2-inhibitors as it was previously observed with other NAH.[21]

Finally, we analyzed the ability of selected hybrid-NAHs to release NO. These were evaluated in the presence of equimolar concentrations of cysteine (Cys) at pH 7.4 and pH 8.3 measuring the NO production during 20 minutes (Table 5). Comparing to the well-known NO-releasing furoxan, derivative **47**,[49] the new hybrid furoxanyl-NAHs displayed lower or null ability to produce NO. Benzofuroxan **15** and furoxans **17** and **42** release small amount of NO under certain conditions. The release of NO could be related to the capabilities to inhibit IL-8 production however no relationship was observed between the rate of NO-releasing (Table 5) and the percentage of inhibition on interleukin-8 release (i.e., compare both values for furoxans **17** and **47**). Additionally, the best hybrid-NAH LOX-inhibitor and good IL-8 release inhibitor, derivative **42**, was the best NO-producer. On the other hand, the in vivo activities seemed to be unrelated to the NO-releasing activities.

2.4. Hybrid furoxanyl-NAHs as drug candidates

In order to confirm NAHs potential as drug candidates, for treatment of different inflammatory diseases, some others experiments were performed. Firstly, hybrid-NAH stability at different pH was studied. Secondly, we studied the mutagenic potential of the compounds using the Ames test.

Table 3
In vitro LOX-inhibition for new selected NAHs and quercetin

Compd	%LOX Inhib [a]/IC_{50} (μM)	Compd	%LOX Inhib [a] / IC_{50} (μM)
13	22 ± 20/ag[b]	**28**	55 ± 10*/~50
14	14 ± 15/>100	**31**	0
15	0/—[c]	**32**	0/—
17	0/>100	**33**	10 ± 4/>100
18	55 ± 11*/~50	**34**	0/—
20	0	**36**	[d]
22	27 ± 28/ag	**37**	37 ± 12/ag
23	[d]	**38**	0/—
24	0/—	**40**	58 ± 23
25	0/—	**41**	1 ± 4/—
		42	74 ± 10**/35 ± 3
		43	55 ± 5*/~50
Quer[e]	35	**44**	53 ± 7*/~50

[a] % of LOX-inhibition at 50 μM doses.
[b] ag: the compound formed aggregates in the buffer, pH 7.4, at doses higher than 50 μM.
[c] —: not determined.
[d] The compound interfered in the assay measurement.
[e] Quer: quercetin, evaluated at 4 μM. *p <0.05, **p <0.01 Student t-test.

Table 4
In vitro COX-1 and COX-2 inhibition assay for new selected NAHs and indomethacin

Compd	Dose (μM)	%COX-1 Inhib [a]	%COX-2 Inhib[a]
17	10	27.0 ± 0.4***	13.1 ± 2.3
	50	28.5 ± 0.1***	11.9 ± 1.7
24	10	25.9 ± 3.6***	19.6 ± 2.1
	50	22.3 ± 0.9***	6.4 ± 2.5
31	10	22.5 ± 0.5***	17.8 ± 1.2*
	50	25.3 ± 0.3***	22.0 ± 1.3*
Ind[e]	0.1	49.7 ± 0.7***	—[c]
	6	—	53.4 ± 9.8**

[a] % of COX-inhibition.
[b] Ind: indomethacin.
[c] —: not determined. *p <0.05, **p <0.01, ***p <0.001. Student t-test.

Table 5
NO releasing rate for new selected NAHs

Compd	NO (nM/min)[a]	
	pH 7.4	pH 8.3
15	0	0.64[b]
17	0	0.39[c]
18	—[d]	0
20	0	0
24	0	0
41	—	0
42	1.04	0.19
44	—	0
47	3700[e]	nd[f]

[a] At 25 °C and NAH:Cys ratio of 1:1.
[b] At 37 °C.
[c] NAH:Cys ratio of 3:1.
[d] —: not determined.
[e] From Ref. 49
[f] nd: not described.

In aqueous solution, at 37 °C, and at different pHs (2.0, 5.0, 7.2, and 8.0) the studied hybrid-NAHs, **13–15**, **17**, **20**, **21**, **27-33**, **36**, **38**, and **42**, were stables during 24 h (evidenced by chromatography) (not shown).

The method of direct incubation in plate[50] using culture of *Salmonella typhimurium* TA98 strain was performed on one furoxan-NAH with in vivo analgesic property, **17**, one benzofuroxan-NAH and one furoxan-NAH with in vivo analgesic and anti-inflammation properties, **24**, and **31**, and the furoxan-NAH with in vitro LOX-inhibition ability, **42**. Except for NAH **31**, the compounds evaluated in this test presented an important capability of inhibition of the NF-κB pathway. The influence of metabolic activation was tested by adding S9 fraction of mouse liver. Positive controls of 4-nitro-*o*-phenylendiamine and 2-aminofluorene were run in parallel. The revertant number was manually counted and compared to the natural revertant (Table 6). The compound is considered mutagenic when the number of revertant colonies is at least twofold of the spontaneous revertant frequencies for at least two consecutive dose levels.[51] The maximum assayed doses were determined according to toxic effect on *S. typhimurium*. The furoxan-NAHs, **17**, **31**, and **42**, were not mutagenic however the benzofuroxan-NAH, **24**, displayed mutagenic effects without S9 fraction and surprisingly this property disappeared after metabolization.

3. Discussion and conclusions

We reported the synthesis and biological evaluation of new hybrid furoxanyl *N*-acylhydrazones as orally effective analgesic and anti-inflammatory agents. The compounds were designed as hybrid entities combining different aromatic residues, between others the furoxan system, connected by *N*-acylhydrazone moiety. Hybrid furoxans **17** and **20** were one of the best in vitro NF-κB pathway inhibitors (Table 1) being at 400 μM 15 and 1.6 times more active than thalidomide, the latest described as a reducing agent for IL-8 production (in vivo NF-κB pathway inhibitor).[52] The corresponding parent hydrazides **45** and **46**, according to GFP expression, displayed not activity on the NF-κB pathway. The benzofuroxan **15** was also one of the best in vitro IL-8 inhibitor being 2 times more active than thalidomide at the lower assayed concentration. Some other hybrid *N*-acylhydrazones, **18**, **19**, **21**, **30**, **38**, **40**, and **42**, at 400 μM displayed similar in vitro activity to thalidomide while derivatives **24**, **28**, **29**, **32**, **33**, **36**, **37**, **41**,

Table 6
Number of revertants of derivatives **17**, **24**, **31**, and **42** on TA98 *S. typhimurium* strain

S9	**17**			**24**			**31**			**42**		
	D[a]	NR[b,c]	M[d]	D[a]	NR[b,c]	M[d]	D[a]	NR[b,c]	M[d]	D[a]	NR[b,c]	M[d]
(−)	0	10 ± 2		0	10 ± 3		0	10 ± 3		0	10 ± 3	
	3.1	8 ± 1		6	10 ± 2		4	11 ± 1		6	5 ± 7	
	9.3	9 ± 4		19	23 ± 2		13	8 ± 3		19	9 ± 1	
	28	10 ± 3		56	30 ± 5	M+[e]	39	17 ± 1		56	11 ± 2	
	83	7 ± 1		167	40 ± 6		117	8 ± 6		167	10 ± 4	
	250	11 ± 1		500	47 ± 9		350	15 ± 4		500	18 ± 5	
(+)	0	8 ± 4		0	11 ± 1		0	11 ± 1		0	11 ± 1	
	3.1	3 ± 1		6	12 ± 7		4	7 ± 1		6	14 ± 4	
	9.3	4 ± 1		19	12 ± 6		13	10 ± 0		19	10 ± 3	
	28	3 ± 1		56	13 ± 1		39	8 ± 3		56	8 ± 1	
	83	12 ± 3		167	17 ± 1		117	5 ± 1		167	9 ± 1	
	250	13 ± 3		500	27 ± 14		350	10 ± 1		500	14 ± 6	

	4-NPD[f]			AF[g]	
	D[c]	NR[d,e]		D[c]	NR[d,e]
−S9	20.0	1900 ± 200	+S9	10.0	844 ± 80

[a] D: doses in μg/plate.
[b] NR: number of revertants.
[c] The results are the means of two independent experiments ±SD.
[d] M: mutagenicity, according to Ref. 51 (see text).
[e] M+: Response is considered positive because it is the second dose in which the revertant levels are at least twice the spontaneous frequencies.
[f] 4-NPD: 4-nitro-*o*-phenylendiamine.
[g] AF: 2-aminofluorene.

and **43** were more effective than thalidomide even at the lowest concentration. Even though the well NO-releasing agent, **47**, inhibited the IL-8 production, the inhibitory effect of our hybrid derivatives on IL-8 production seems not to be related to NO-production (Table 5). From a chemical point of view our best NF-κB pathway/IL-8 releasing inhibitors, **15**, **17**, **20**, **24**, and **43**, share with some previously described inhibitors (**48–50**, Fig. 3)[53] several structural motives, that is, trifluorophenyl-substituted, and aza-heterocyclic carboxamide/imide- or benzo[*d*][1,3]dioxole-arylic substituted.

The toxicity of the new derivatives against murine macrophages was studied (Table 1) finding a wide range of behaviors. In general, the methylfuroxan derivatives, NHA **28–44**, showed lower toxicities than the rest of the studied hybrid compounds. This information together with IL-8 production inhibition was used to select the *N*-acylhydrazones to be evaluated *in vivo*. Accordingly, we included in the in vivo assays the best IL-8 release inhibitors **17**, and **20**, with low macrophage-IC_{50}s, the good IL-8 inhibitors **15**, **24**, **28**, and **33**, with high macrophage-IC_{50}s, the good IL-8 inhibitors **32**, and **36**, with low macrophage-IC_{50}s, and the moderate IL-8 inhibitors **38**, and **42**, with high macrophage-IC_{50}s. Additionally, an in vitro non IL-8 inhibitor was included in the in vivo assay, derivative **31**. Compounds **24** and **31** were the best developed hybrid NAHs that display both analgesic and anti-inflammatory activities when they were administered orally (Table 2). Compounds **20**, **28**, and **36** exhibited moderate analgesic and anti-inflammatory properties. On the other hand, derivatives **15** and **17** at 30 min and **32** and **38** at 60 min displayed relevant in vivo analgesic properties. Furthermore derivatives **17** and **24** were able to modestly reduce inflammatory nociception between 0.5 and 3 h (Fig. 1) and the analgesic property of derivative **31** was maintained between 1 to 4 h ca. 20% (Fig. 2). These data agree with the in vitro inhibition of the NF-κB pathway.

Apart from IL-8 inhibition, mechanism of in vivo analgesia and anti-inflammation, additional biochemical pathways were studied including inhibition of LOX, COX-1, and COX-2. The in vivo active derivatives **17**, **24**, and **31** did not inhibit COXs at the indomethacin level however some degree of better inhibition of COX-1 than COX-2 were displayed (Table 4). Derivatives **17**, **24**, and **31** did not inhibit LOX at the quercetin level (Table 3). In reference to LOX-inhibition (Table 3), derivative **42** appeared as a structural hit to develop new inhibitors of this enzyme, also hybrid-NAHs **18**, **28**, **43**, and **44** could be considered.

In line with these findings, furoxans **17**, **31**, and **42** were not mutagenic in the Ames test (Table 6), making them excellent leads for further studies. However, the benzofuroxan **24** resulted mutagenic in absence of S9 fraction which does not justify, at least initially, additional studies.

These findings prompt us to deepen our studies, modifying doses, administration routes, and combinations with other drugs.

4. Experimental

Reagents were purchased from Aldrich and used without further purification. Melting points were performed using an Electrothermal Engineering Ltd melting point apparatus, and the results were uncorrected. Infrared spectra were recorded on a Bomem FTLA2000 spectrophotometer instrument as films on KBr discs. ^{1}H and ^{13}C NMR spectra were recorded in the indicated solvent on Bruker DX 400 MHz spectrometer. Chemical shifts are quoted in parts per million downfield from TMS and the coupling constants are in Hertz. Mass spectra were recorded on a Hewlett Packard MSD 5973 (electronic impact, EI) or on a Hewlett Packard LC/MS Series 1100 (electrospray ionization, ESI) instruments. All solvents were dried and distilled prior to use. All the reactions were carried out in a nitrogen atmosphere. Reactions were monitored by TLC using commercially available precoated plates (Merck Kieselgel 60 F254 silica) and developed plates were examined under UV light (254 nm) or as iodine vapor stains. Column chromatography was performed using 200 mesh silica gel. To determine the purity of the compounds, microanalyses were done on a Fisons EA 1108 CHNS–O instrument from vacuum-dried samples and were within ±0.4 of the values obtained by calculated compositions. Compounds (**I**)–(**III**), benzo[*d*][1,3]dioxole-5-carbohydrazide, 2-methyl-4*H*-imidazo[1,2-*a*]pyridine-3-carbohydrazide, 5-methyl-1*H*-imidazole-4-carbohydrazide, and 1-phenyl-1*H*-pyrazole-4-carbohydrazide were prepared following synthetic procedures previously reported.[27,28,40–43,54–56]

4.1. Nicotinohydrazide

A mixture of nicotinic acid (3 g, 24 mmol), MeOH (60 mL) and H_2SO_4 (c) (12 mL) was heated at reflux for 1.5 h. The MeOH was distilled at reduced pressure and the residue was dissolved AcOEt (50 mL) and washed with saturated aqueous solution of $NaHCO_3$ (3 × 10 mL). The organic phase was dried with anhydrous Na_2SO_4 and evaporated under reduced pressure. The residue, methyl nicotinate (white solid, 2.7 g, 83%), was used in the next step without purification. A mixture of methyl nicotinate (2.7 g, 20 mmol),

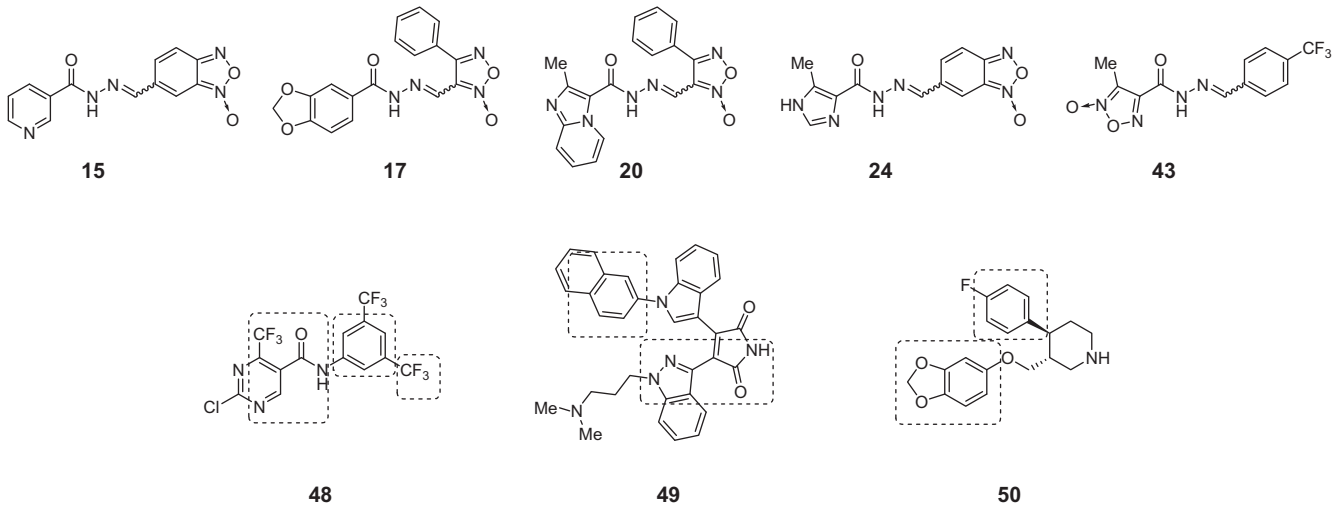

Figure 3. Structural scaffolds (dotted squares) shared by some IL-8-production inhibitors and our hybrid-NAHs.

MeOH (4 mL) and $NH_2NH_2{\cdot}H_2O$ (98%, 0.95 mL) was heated at reflux for 6.5 h. The white solid, nicotinohydrazide, was filtered and washed several times with cold EtOH (1.8 g, 67%).

4.1.1. General procedure for the synthesis of compounds 13–15

To a solution of nicotinohydrazide (150 mg, 1.1 mmol) in dry EtOH (2.5 mL) was added the corresponding aldehyde ((**I**), (**II**), or (**III**), 0.9 mmol) and a drop of glacial AcOH. The mixture was stirred until the aldehyde was consumed (checked by TLC). The solid precipitated was filtered and washed with cold EtOH.

4.1.1.1. *N*′-(2-Methyl-3-furoxanylmethylidene)nicotinohydrazide (13). (*E*/*Z* proportion = 95:5). White solid (46%). *E*-isomer: ^{1}H NMR (DMSO-d_6) δ ppm: 2.41 (3H, s), 7.63 (1H, d, J = 8.0), 8.28 (1H, d, J = 8.0), 8.48 (1H, s), 8.91 (1H, s), 9.09 (1H, s), 12.56 (1H, s). ^{13}C NMR (DMSO-d_6) δ ppm: 9.6, 112.2, 124.3, 128.9, 136.1, 137.3, 149.1, 153.3, 154.5, 162.6, 207.0. IR (KBr) υ (cm^{-1}): 3205, 1703, 1604, 1565, 1271, 1024, 853, 795. MS (ESI) *m*/*z* (%): 248 (M^++H, 100), 106 (M^+−141, 1). Calcd analysis for $C_{10}H_9N_5O_3$: C: 48.6; H: 3.7; N: 28.3. Found: C: 48.5; H: 3.4; N: 27.9.

4.1.1.2. *(E)*-*N*′-(4-Phenyl-3-furoxanylmethylidene)nicotinohydrazide (14). Yellow solid (24%); mp: 159.7–162.8 °C. ^{1}H NMR (DMSO-d_6) δ ppm: 7.35 (1H, s), 7.59 (2H, d, J = 8.0), 7.98 (2H, d, J = 8.0), 8.16 (1H, d, J = 8.0), 8.37 (1H, s), 8.81 (1H, d, J = 4.0), 9.07 (1H, s), 12.44 (1H, s). ^{13}C NMR (DMSO-d_6) δ ppm: 113.3, 124.2, 126.1, 129.5, 131.8, 134.2, 135.1, 136.0, 149.2, 152.3, 153.2, 156.5, 162.2. IR (KBr) υ (cm^{-1}): 3242, 1667, 1587, 1557, 1298, 1022, 858, 820. MS (ESI) *m*/*z* (%): 310 (M^++H, 100). Calcd analysis for $C_{15}H_{11}N_5O_3$: C: 58.2; H: 3.6; N: 22.6. Found: C: 57.9; H: 3.7; N: 22.7.

4.1.1.3. *(E)*-*N*′-(5-Benzofuroxanylmethylidene)nicotinohydrazide (15). Yellow solid (74%); mp: 195.3–198.6 °C. ^{1}H NMR (DMSO-d_6) δ ppm: 7.59 (1H, dd, J_1 = 4.0 Hz, J_2 = 4.0 Hz), 7.49–8.29 (3H, br m), 8.28 (1H, d, J = 8.0), 8.50 (1H, s), 8.79 (1H, s), 9.09 (1H, s), 12.38 (1H, s). ^{13}C NMR (DMSO-d_6) δ ppm: 114.0, 119.0, 124.2, 129.3, 131.0, 136.1, 142.5, 146.2, 149.2, 153.0, 162.6. IR (KBr) υ (cm^{-1}): 3219, 1657, 1603, 1572, 1528, 1295, 1014, 828, 800. MS (ESI) *m*/*z* (%): 284 ($M^{+\cdot}$+H, 100), 268 ($M^{+\cdot}$+H-16, 1), 178 ($M^{+\cdot}$-106, 1). Calcd analysis for $C_{13}H_9N_5O_3$: C: 55.1; H: 3.2; N: 24.7. Found: C: 55.0; H: 2.9; N: 24.4.

4.2. General procedure for the synthesis of compounds 16–18

To a solution of benzo[*d*][1,3]dioxole-5-carbohydrazide (250 mg, 1.4 mmol) in dry toluene (5 mL) was added the corresponding aldehyde ((**I**), (**II**), or (**III**), 1.3 mmol) and a drop of glacial AcOH. The mixture was stirred until the aldehyde was consumed (checked by TLC). The product was purified as is indicated below.

4.2.1. *(E)*-*N*′-(2-Methyl-3-furoxanylmethylidene)benzo[*d*][1,3]dioxole-5-carbohydrazide (16)

The solid precipitated was filtered and washed with cold toluene. Light yellow solid (86%); mp: 189.4–192.0 °C. ^{1}H NMR (DMSO-d_6) δ ppm: 2.39 (3H, s), 6.13 (2H, s), 7.08 (1H, d, J = 8.0), 7.45 (1H, s), 7.54 (1H, d, J = 8.0), 8.45 (1H, s), 12.25 (1H, s). ^{13}C NMR (DMSO-d_6) δ ppm: 9.7, 102.3, 108.2, 108.7, 112.2, 123.7, 123.7, 148.1, 150.0, 154.6, 136.1, 151.2, 162.9. IR (KBr) υ (cm^{-1}): 3200, 1648, 1570, 1613, 1259, 1169, 1125, 1069, 1034, 929, 857, 801. MS (EI) *m*/*z* (%): 290 (M^+, 2), 149 (100), 121 (15), 65 (12). Calcd analysis for $C_{12}H_{10}N_4O_5$: C: 49.7; H: 3.5; N: 19.3. Found: C: 49.6; H: 3.3; N: 19.2.

4.2.2. *(E)*-*N*′-(4-Phenyl-3-furoxanylmethylidene)benzo[*d*][1,3]dioxole-5-carbohydrazide (17)

The solvent of reaction was evaporated in vacuo and the residue was purified by column chromatography (SiO_2, CH_2Cl_2:MeOH (0 to 5%)). White solid (56%); mp: 196.3–198.1 °C. ^{1}H NMR (DMSO-d_6) δ ppm: 6.13 (2H, s), 7.07 (1H, d, J = 8.0), 7.43 (1H, s), 7.50 (1H, m), 7.58 (4H, m), 7.62 (3H, m), 7.98 (2H, m), 8.35 (1H, s), 12.14 (1H, s). ^{13}C NMR (DMSO-d_6) δ ppm: 102.5, 108.0, 108.5, 113.5, 123.5, 126.0, 127.0, 129.0, 129.5, 131.5, 132.5, 148.0, 151.0, 157.0. IR (KBr) υ (cm^{-1}): 3219, 1658, 1565, 1565, 1504, 1262, 1173, 1117, 1083, 1041, 929, 874, 842. MS (EI) *m*/*z* (%): 352 (M^+, 1), 149 (100), 121 (26), 77 (9). Calcd analysis for $C_{17}H_{12}N_4O_5$: C: 58.0; H: 3.4; N: 15.9. Found: C: 57.8; H: 3.3; N: 15.6.

4.2.3. *(E)*-*N*′-(5-Benzofuroxanylmethylidene)benzo[*d*][1,3]dioxole-5-carbohydrazide (18)

The solid precipitated was filtered and washed with cold toluene. Yellow solid (98%); mp: 220.4–221.8 °C. ^{1}H NMR (DMSO-d_6) δ ppm: 6.14 (2H, s), 7.07 (1H, d, J = 8.0), 7.47 (1H, s), 7.55 (1H, d, J = 8.0), 7.85–8.12 (3H, m), 8.47 (1H, s), 12.08 (1H, s). ^{13}C NMR (DMSO-d_6) δ ppm: 102.4, 108.2, 108.6, 113.7, 118.0, 123.6, 127.1, 129.9, 145.0, 147.9, 150.9, 162.9. IR (KBr) υ (cm^{-1}): 3222, 1649, 1614, 1572, 1551, 1257, 1171, 1110, 1062, 1031, 929, 857. MS (EI) *m*/*z* (%): 326 (M^+, 1), 149 (100), 121 (27), 65 (50). Calcd analysis for $C_{15}H_{10}N_4O_5$: C: 55.2; H: 3.1; N: 17.2. Found: C: 55.0; H: 3.1; N: 17.1.

4.3. General procedure for the synthesis of compounds 19–21

To a solution of 2-methyl-4*H*-imidazo[1,2-*a*]pyridine-3-carbohydrazide (1 equiv) in dry EtOH (5 mL/mmol of hydrazide) was added the corresponding aldehyde ((**I**), (**II**), or (**III**), 0.9 equiv) and a drop of glacial AcOH. The mixture was stirred until the aldehyde was consumed (checked by TLC). The product was purified as is indicated below.

4.3.1. *(E)*-2-Methyl-*N*′-(2-methyl-3-furoxanylmethylidene)-4*H*-imidazo[1,2-*a*]pyridine-3-carbohydrazide (19)

The solid precipitated was filtered and washed with cold EtOH. Yellow solid (81%); mp: 165.9–167.4 °C. ^{1}H NMR (DMSO-d_6) δ ppm: 2.26 (3H, s), 2.53 (3H, s), 7.07 (1H, t, J = 4.0), 7.45 (1H, t, J = 4.0), 7.65 (1H, d, J = 8.0), 8.40 (1H, s), 8.91 (1H, d, J = 8.0), 12.01 (1H, s). ^{13}C NMR (DMSO-d_6) δ ppm: 9.4, 16.3, 114.0, 115.0, 116.7, 127.8, 128.1, 135.6, 154.4, 159.3. IR (KBr) υ (cm^{-1}): 3184, 1660, 1610, 1573, 1339, 1296, 1229, 1014, 865, 802. MS (EI) *m*/*z* (%): 300 (M^+, 5), 201 (2), 159 (100), 90 (19). Calcd analysis for $C_{13}H_{12}N_6O_3$: C: 52.0; H: 4.0; N: 28.0. Found: C: 51.9; H: 3.9; N: 27.8.

4.3.2. *(E)*-2-Methyl-*N*′-(4-phenyl-3-furoxanylmethylidene)-4*H*-imidazo[1,2-*a*]pyridine-3-carbohydrazide (20)

The solvent of reaction was evaporated in vacuo and the residue was purified by column chromatography (SiO_2, CH_2Cl_2:MeOH (0 to 10%)). White solid (12%); mp: 184.2–186.6 °C. ^{1}H NMR (DMSO-d_6) δ ppm: 2.51 (s, 3H), 7.01 (t, 1H, J = 8.1), 7.25–7.65 (m, 6H), 7.87 (d, 1H, J = 8.1), 8.24 (s, 1H), 8.84 (d, 1H, J = 8.1), 11.92 (s, 1H). ^{13}C NMR (DMSO-d_6) δ ppm: 40.0, 113.5, 115.0, 117.0, 128.0, 129.0, 129.0, 131.0, 132.0, 146.0, 147.0, 148.0, 156.0. IR (KBr) υ (cm^{-1}): 3226, 1681, 1634, 1337, 1293, 1212, 1047, 845, 753. MS (EI) *m*/*z* (%): 332 (M^+ 30, 4), 159 (100), 131 (10). Calcd analysis for $C_{18}H_{14}N_6O_3$: C: 59.7; H: 3.9; N: 23.2. Found: C: 59.5; H: 3.7; N: 23.2.

4.3.3. *(E)*-*N*′-(5-Benzofuroxanylmethylidene)-2-methyl-4*H*-imidazo[1,2-*a*]pyridine-3-carbohydrazide (21)

The solid precipitated was filtered and washed with cold EtOH. Yellow solid (87%); mp: 263.9 (d). ^{1}H NMR (DMSO-d_6) δ ppm: 2.52 (3H, s), 7.09 (1H, t, J = 4.0), 7.46 (1H, t, J = 8.0), 7.64 (1H, d, J = 8.0), 7.63–8.19 (3H, bs), 8.40 (1H, s), 8.89 (1H, d, J = 8.0), 11.88 (1H, s). ^{13}C NMR (DMSO-d_6) δ ppm: 113.8, 116.7, 127.7, 135.0, 144.0,

161.0. IR (KBr) υ (cm^{-1}): 3200, 1647, 1620, 1344, 1297, 1231, 1012, 862, 757. MS (EI) *m/z* (%): 336 ($M^{+\cdot}$, 2), 320 (1), 159 (100), 90 (35). Calcd analysis for $C_{16}H_{12}N_6O_3$: C: 57.1; H: 3.6; N: 25.0. Found: C: 57.1; H: 3.3; N: 25.3.

4.4. General procedure for the synthesis of compounds 22–24

To a solution of 5-methyl-1*H*-imidazole-4-carbohydrazide (1 equiv) in dry EtOH (2.5 mL/mmol of hydrazide) was added the corresponding aldehyde (**(I)**, **(II)**, or **(III)**, 0.9 equiv) and a drop of glacial AcOH. The mixture was stirred until the aldehyde was consumed (checked by TLC). The solid precipitated was filtered and washed with cold EtOH.

4.4.1. *(E)*-5-Methyl-*N′*-(2-methyl-3-furoxanylmethylidene)-1*H*-imidazole-4-carbohydrazide (22)

White solid (40%); mp: 190.1–192.3 °C. ^{1}H NMR (DMSO-d_6) δ ppm: 2.39 (3H, s), 2.49 (1H, s), 7.70 (1H, s), 8.59 (1H, s), 12.15 (1H, s), 12.58 (1H, s). ^{13}C NMR (DMSO-d_6) δ ppm: 9.7, 112.3, 128.0, 134.4, 134.8, 155.0, 160.3. IR (KBr) υ (cm^{-1}): 3200, 1652, 1599, 1538, 1305, 1039, 863, 800. MS (ESI) *m/z* (%): 251 ($M^{+\cdot}$+H, 100), 141 (2), 109 (7). Calcd analysis for $C_9H_{10}N_6O_3$: C: 43.2; H: 4.0; N: 33.6. Found: C: 43.4; H: 3.8; N: 33.3.

4.4.2. *(E)*-5-Methyl-*N′*-(4-phenyl-3-furoxanylmethylidene)-1*H*-imidazole-4-carbohydrazide (23)

White solid (14%); mp: 226.8–229.5 °C. ^{1}H NMR (DMSO-d_6) δ ppm: 2.47 (3H, s), 7.56–7.63 (3H, m), 7.67 (1H, s), 7.98 (2H, d, *J* = 8.0), 8.48 (1H, s), 12.09 (1H, s), 12.59 (1H, s). ^{13}C NMR (DMSO-d_6) δ ppm: 11.0, 113.5, 126.3, 129.0, 129.2, 129.6, 131.6, 134.0, 134.2, 156.5, 160.1. IR (KBr) υ (cm^{-1}): 3097, 1660, 1595, 1559, 1512, 1244, 1039, 863, 800. MS (ESI) *m/z* (%): 313 (M^{+}+H, 100). Calcd analysis for $C_{14}H_{12}N_6O_3$: C: 53.8; H: 3.9; N: 26.9. Found: C: 53.7; H: 3.7; N: 26.7.

4.4.3. *(E)-N′*-(5-Benzofuroxanylmethylidene)-5-methyl-1*H*-imidazole-4-carbohydrazide (24)

Yellow solid (76%); mp: 229.7–231.8 °C. ^{1}H NMR (DMSO-d_6) δ ppm: 2.45 (3H, s), 7.52–8.12 (4H, m), 8.55 (1H, s), 11.74 (1H, s), 12.55 (1H, s). ^{13}C NMR (DMSO-d_6) δ ppm: 11.1, 113.0, 119.0, 129.1, 130.2, 133.5, 134.2, 143.9, 160.3. IR (KBr) υ (cm^{-1}): 3137, 1657, 1603, 1518, 1295, 1015, 893, 805. MS (ESI) *m/z* (%): 287 ($M^{+\cdot}$+H, 100), 205 (1), 109 (3). Calcd analysis for $C_{12}H_{10}N_6O_3$: C: 50.3; H: 3.5; N: 29.4. Found: C: 50.1; H: 3.4; N: 29.1.

4.5. General procedure for the synthesis of compounds 25–27

To a solution of 1-phenyl-1*H*-pyrazole-4-carbohydrazide (1 equiv) in dry EtOH (5 mL/mmol of hydrazide) was added the corresponding aldehyde (**(I)**, **(II)**, or **(III)**, 0.9 equiv) and a drop of glacial AcOH. The mixture was stirred until the aldehyde was consumed (checked by TLC). The solid precipitated was filtered and washed with cold EtOH.

4.5.1. *N′*-(2-Methyl-3-furoxanylmethylidene)-1-phenyl-1*H*-pyrazole-4-carbohydrazide (25)

(*E*/*Z* proportion = 67:33). White solid (23%). *E*-isomer: ^{1}H NMR (DMSO-d_6) δ ppm: 2.40 (1H, s), 7.40 (1H, t, *J* = 8.0), 7.56 (2H, t, *J* = 8.0), 7.92 (2H, d, *J* = 8.0), 8.29 (1H, s), 8.42 (1H, s), 9.10 (1H, s), 12.22 (1H, s). ^{13}C NMR (DMSO-d_6) δ ppm: 9.6, 112.2, 118.6, 119.4, 127.8, 130.2, 130.6, 135.5, 139.4, 140.9, 154.6. IR (KBr) υ (cm^{-1}): 1635, 1503, 1224, 1013, 870, 821. MS (EI) *m/z* (%): 312 (M^{+}, 1), 213 (2), 171 (100), 77 (17). Calcd analysis for $C_{14}H_{12}N_6O_3$: C: 53.8; H: 3.9; N: 26.9. Found: C: 53.6; H: 3.8; N: 26.7.

4.5.2. *(E)*-1-Phenyl-*N′*-(4-phenyl-3-furoxanylmethylidene)-1*H*-pyrazole-4-carbohydrazide (26)

Gray solid (80%); mp: 200.2–202.3 °C. ^{1}H NMR (DMSO-d_6) δ ppm: 7.43 (1H, t, *J* = 8.0), 7.59 (5H, d, *J* = 12.0), 7.77 (2H, d, *J* = 8.0), 7.84 (2H, d, *J* = 8.0), 8.02 (1H, s), 8.26 (1H, s), 9.18 (1H, s), 11.96 (1H, s). ^{13}C NMR (DMSO-d_6) δ ppm: 112.7, 117.0, 119.3, 126.0, 127.8, 128.3, 129.0, 129.7, 130.5, 131.8, 139.5, 147.7, 156.9, 163.0. IR (KBr) υ (cm^{-1}): 3165, 1658, 1599, 1544, 1503, 1206, 1036, 874, 751. MS (EI) *m/z* (%): 171 ($M^{+\cdot}$-203, 100), 77 (90). Calcd analysis for $C_{19}H_{14}N_6O_3$: C: 61.0; H: 3.8; N: 22.4. Found: C: 60.8; H: 3.6; N: 22.4.

4.5.3. *(E)-N′*-(5-Benzofuroxanylmethylidene)-1-phenyl-1*H*-pyrazole-4-carbohydrazide (27)

Yellow solid (21%); mp: 210.0–212.0 °C. ^{1}H NMR (DMSO-d_6) δ ppm: 7.42 (1H, t, *J* = 8.0), 7.51–7.93 (3H, br m), 7.53 (2H, t, *J* = 8.0), 7.85 (2H, d, *J* = 8.0), 8.14 (1H, s), 8.18 (1H, s), 8.90 (1H, s), 12.04 (1H, s). ^{13}C NMR (DMSO-d_6) δ ppm: 113.5, 119.4, 127.8, 130.1, 139.5, 141.0, 142.2, 144.3, 162.0. IR (KBr) υ (cm^{-1}): 3252, 1658, 1620, 1564, 1530, 1281, 1012, 882, 758. MS (EI) *m/z* (%): 171 ($M^{+\cdot}$-177, 100), 77 (26). Calcd analysis for $C_{17}H_{12}N_6O_3$: C: 58.6; H: 3.5; N: 24.1. Found: C: 58.5; H: 3.7; N: 24.3.

4.6. 3-Methylfuroxan-4-carbohydrazide (IV)

To a solution of (**I**) (1 g, 7.8 mmol) in MeOH (12 mL) stirred at 0 °C was added subsequently KCN (839 mg, 12.9 mmol) and finally MnO_2 (3.392 g, 39 mmol) in small portions over 5 min. The reaction was stirred for 30 minutes at 0 °C and then it was filtered through a Celite column and the Celite was washed three times with CH_2Cl_2 (15 mL each). The organic phase was washed with brine, dried with anhydrous Na_2SO_4 and evaporated in vacuo to yield methyl 3-methylfuroxan-4-carboxylate as light brown oil (597 mg, 48%). ^{1}H NMR (DMSO-d_6) δ ppm: 2.40 (s, 3H), 4.06 (s, 3H). ^{13}C NMR (DMSO-d_6) δ ppm: 8.0, 53.0, 110.0, 149.0, 159.0. The ester was used without further purification in the next step. To a solution of methyl 3-methyl-4-furoxancarboxylate (597 mg, 3.8 mmol) in EtOH (10 mL) stirred at 0 °C was added $NH_2NH_2{\cdot}H_2O$ (70%, 0.13 mL). The reaction mixture was stirred for 1 h and then the solvent was evaporated in vacuo and the residue was treated with EtOAc (150 mL) and washed with brine. The organic phase was dried with anhydrous Na_2SO_4 and evaporated in vacuo. The product **(IV)**, as a light brown oil (484 mg, 81%), was used without purification in the next reactions.

4.6.1. General procedure for the synthesis of compounds 28–43

To a solution of (**IV**) (1 equiv) in dry toluene (5 mL/mmol of hydrazide) was added the corresponding aldehyde (0.9 equiv) and a drop of glacial AcOH. The mixture was stirred until the aldehyde was consumed (checked by TLC). The solid precipitated was filtered and washed with cold toluene.

4.6.1.1. *(E)*-3-Methyl-*N′*-(2-methyl-3-furoxanylmethylidene) furoxan-4-carbohydrazide (28). Yellow solid (51%); mp: 150.4–152.0 °C. ^{1}H NMR (DMSO-d_6) δ ppm: 2.40 (s, 3H), 2.48 (s, 3H), 8.75 (s, 1H), 11.98 (s, 1H). ^{13}C NMR (DMSO-d_6) δ ppm: 7.5, 8.0, 112.0, 113.0, 138.0, 151.0, 154.0, 155.0. IR (KBr) υ (cm^{-1}): 3206, 1719, 1616, 1598, 1560, 1234, 1044, 864, 800. MS (EI) *m/z* (%): 268 (M^{+} 6), 208 (5), 169 (11), 143 (16), 125 (2). Calcd analysis for $C_8H_8N_6O_5$: C: 35.8; H: 3.0; N: 31.3. Found: C: 35.6; H: 3.1; N: 31.2.

4.6.1.2. *(E)*-3-Methyl-*N′*-(4-phenyl-3-furoxanylmethylidene) furoxan-4-carbohydrazide (29). White solid (14%); mp: 185.0–189.0 °C. ^{1}H NMR (DMSO-d_6) δ ppm: 2.29 (3H, s), 7.36 (1H, d, *J* = 8.0), 7.64 (2H, d, *J* = 8.0), 7.91 (2H, d, *J* = 8.0), 8.46 (1H,

s), 12.98 (1H, s). ^{13}C NMR (DMSO-d_6) δ ppm: 8.9, 113.1, 113.4, 126.0, 129.0, 129.0, 129.2, 129.5, 136.3, 151.6, 154.2, 156.6. IR (KBr) υ (cm^{-1}): 1727, 1611, 1561, 1541, 1221, 1048, 866, 843. MS (EI) *m/z* (%): 330 (M$^+$ 2), 314 (1), 231 (2), 127 (47), 67 (100). Calcd analysis for $C_{13}H_{10}N_6O_5$: C: 47.3; H: 3.0; N: 25.4. Found: C: 47.5; H: 3.1; N: 25.3.

4.6.1.3. *(E)*-*N* ′-(5-Benzofuroxanylmethylidene)-3-methylfuroxan-4-carbohydrazide (30). Brown solid (32%); mp: 107.9–109.3 °C. ^{1}H NMR (DMSO-d_6) δ ppm: 2.41 (3H, s), 7.10–7.29 (1H, br s), 7.60–7.90 (2H, m), 8.72 (1H, s), 10.09 (1H, s). IR (KBr) υ (cm^{-1}): 1616, 1468, 1250. MS (EI) *m/z* (%): 304 (M$^+$ 20), 288 (5), 205 (7), 67 (100). Calcd analysis for $C_{11}H_8N_6O_5$: C: 43.4; H: 2.6; N: 27.6. Found: C: 43.2; H: 2.7; N: 27.4.

4.6.1.4. *(E)*-*N* ′-(4-Dimethylaminophenylmethylidene)-3-methylfuroxan-4-carbohydrazide (31). Yellow solid (54%); mp: 183.0–185.0 °C. ^{1}H NMR (acetone-d_6) δ ppm: 2.38 (s, 3H), 3.05 (s, 6H), 6.80 (2H, d, J = 9.0), 7.64 (2H, d, J = 9.0), 8.44 (s, 1H), 11.05 (s, 1H). ^{13}C NMR (acetone-d_6) δ ppm: 8.1, 39.7, 112.1, 112.9, 121.8, 129.4, 151.4, 152.0, 152.7, 153.5. IR (KBr) υ (cm^{-1}): 3100, 1605, 1605, 1553, 1526, 1258, 1034, 839, 825. MS (EI) *m/z* (%): 289 (M$^+$ 100), 175 (89), 146 (68), 133 (50), 118 (36). Calcd analysis for $C_{13}H_{15}N_5O_3$: C: 54.0; H: 5.2; N: 24.2. Found: C: 53.8; H: 5.0; N: 23.9.

4.6.1.5. *(E)*-*N*′-(4-Bromophenylmethylidene)-3-methylfuroxan-4-carbohydrazide (32). White solid (56%); mp: 175.2–182.0 °C. ^{1}H NMR (acetone-d_6) δ ppm: 2.39 (s, 3H), 7.68 (2H, d, J = 8.5), 7.67 (2H, d, J = 8.5), 8.60 (s, 1H), 11.43 (s, 1H). ^{13}C NMR (acetone-d_6) δ ppm: 8.1, 113.0, 124.7, 129.6, 132.4, 133.9, 149.4, 152.0. IR (KBr) υ (cm^{-1}): 3200, 1683, 1615, 1469, 1259, 1038, 896, 827, 652. MS (EI) *m/z* (%): 326/324 (M$^+$ 12), 227/225 (21), 198/196 (6), 183/181 (36), 170/168 (11), 157/155 (20), 143 (17), 118 (34), 89 (77), 67 (100), 57 (5). Calcd analysis for $C_{11}H_9BrN_4O_3$: C: 40.6; H: 2.8; N: 24.6. Found: C: 40.7; H: 2.6; N: 24.3.

4.6.1.6. *(E)*-3-Methyl-*N*′-(thiophen-2-ylmethylidene)furoxan-4-carbohydrazide (33). White solid (54%); mp: 179.3–183.7 °C. ^{1}H NMR (acetone-d_6) δ ppm: 2.39 (s, 3H), 7.17 (dd, 1H, J_1 = 4.9, J_2 = 3.8), 7.49 (d, 1H, J = 3.7), 7.67 (d, 1H, J = 5.1), 8.84 (s, 1H), 11.33 (s, 1H). ^{13}C NMR (acetone-d_6) δ ppm: 12.0, 108.0, 127.0, 130.0, 137.0, 145.0, 158.0, 170.0. IR (KBr) υ (cm^{-1}): 3096, 1672, 1614, 1593, 1566, 1256, 1042, 883, 843, 731. MS (EI) *m/z* (%): 252 (M$^+$ 53), 153 (65), 143 (11), 109 (76), 96 (51), 83 (25), 67 (100), 57 (13). Calcd analysis for $C_9H_8N_4O_3S$: C: 42.8; H: 3.2; N: 22.2; S: 12.7. Found: C: 42.6; H: 2.9; N: 21.9; S: 12.5.

4.6.1.7. *(E)*-*N*′-(2-Furylmethylidene)-3-methylfuroxan-4-carbohydrazide (34). White solid (28%); mp: 179.5 °C (d). ^{1}H NMR (acetone-d_6) δ ppm: 2.39 (s, 3H), 6.64 (1H, dd, J_1 = 1.8, J_2 = 1.6), 6.97 (1H, d, J = 3.4), 7.68 (1H, s), 8.52 (1H, s), 11.33 (1H, s). ^{13}C NMR (acetone-d_6) δ ppm: 8.1, 112.5, 113.0, 114.3, 140.2, 145.8, 150.0, 152.0, 154.0. IR (KBr) υ (cm^{-1}): 3130, 1684, 1615, 1582, 1259, 1038, 879, 843. MS (EI) *m/z* (%): 236 (M$^+$ 43), 220 (3), 143 (5), 137 (72), 93 (40), 81 (28), 67 (100), 57 (6). Calcd analysis for $C_9H_8N_4O_4$: C: 45.8; H: 3.4; N: 23.7. Found: C: 45.5; H: 3.2; N: 23.5.

4.6.1.8. *(E)*-3-Methyl-*N* ′-(5-nitrothiophen-2-ylmethylidene) furoxan-4-carbohydrazide (35). White solid (45%); mp: 191.0 °C (d). ^{1}H NMR (acetone-d_6) δ ppm: 2.34 (3H, s), 7.56 (1H, d, J = 4.3), 8.05 (1H, d, J = 4.3), 8.88 (1H, s), 11.76 (1H, s). ^{13}C NMR (acetone-d_6) δ ppm: 8.0, 112.5, 128.0, 129.0, 143.0, 146.0, 152.0, 153.0. IR (KBr) υ (cm^{-1}): 3168, 1677, 1609, 1600, 1538, 1508, 1317, 1253, 1031, 883, 847, 817. MS (EI) *m/z* (%): 297 (M$^+$ 17), 198 (44), 191 (2), 143 (9), 67 (100). Calcd analysis for $C_9H_7N_5O_5S$: C: 36.4; H: 2.4; N: 23.6; S: 10.8. Found: C: 36.1; H: 2.1; N: 23.5; S: 11.0.

4.6.1.9. *(E)*-3-Methyl-*N* ′-(5-nitro-2-furylmethylidene)furoxan-4-carbohydrazide (36). Yellow solid (55%); mp: 197.0–198.6 °C. ^{1}H NMR (acetone-d_6) δ ppm: 2.40 (s, 3H), 7.27 (d, 1H, J = 3.5), 7.64 (d, 1H, J = 3.4), 8.64 (s, 1H), 11.78 (s, 1H). ^{13}C NMR (acetone-d_6) δ ppm: 12.0, 112.0, 113.0, 119.0, 137.0, 151.0, 152.0, 154.0. IR (KBr) υ (cm^{-1}): 3092, 1688, 1621, 1568, 1521, 1353, 1308, 1248, 1038, 887, 815. MS (EI) *m/z* (%): 281 (M$^+$ 12), 221 (8), 182 (28), 154 (20), 67 (100), 57 (17). Calcd analysis for $C_9H_7N_5O_6$: C: 38.4; H: 2.5; N: 24.9. Found: C: 38.2; H: 2.3; N: 24.6.

4.6.1.10. *(E)*-*N* ′-(2-Hydroxyphenylmethylidene)-3-methylfuroxan-4-carbohydrazide (37). White solid (70%); mp: 206.0–218.0 °C. ^{1}H NMR (acetone-d_6) δ ppm: 2.41 (3H, s), 6.97 (1H, t, J = 7.5), 6.99 (1H, d, J = 8.2), 7.37–7.44 (2H, m), 8.76 (1H, s), 11.25 (1H,s), 11.72 (1H, s). ^{13}C NMR (acetone-d_6) δ ppm: 8.1, 112.8, 117.3, 118.1, 119.8, 131.8, 132.5, 151.3, 153.0, 153.9, 159.2. IR (KBr) υ (cm^{-1}): 3586, 3158, 1680, 1620, 1559, 1506, 1248, 1037, 870, 845. MS (EI) *m/z* (%): 262 (M$^+$ 44), 163 (57), 143 (6), 135 (14), 119 (53), 67 (94), 57 (100). Calcd analysis for $C_{11}H_{10}N_4O_4$: C: 50.4; H: 3.8; N: 21.4. Found: C: 50.6; H: 3.6; N: 21.3.

4.6.1.11. *(E)*-*N*′-(3,4-Dimethoxyphenylmethylidene)-3-methylfuroxan-4-carbohydrazide (38). White solid (55%); mp: 193.0–195.2 °C. ^{1}H NMR (DMSO-d_6) δ ppm: 2.27 (3H, s), 3.87 (6H, s), 7.02 (1H, d, J = 8.1), 7.23 (1H, d, J = 8.1), 7.34 (1H, s), 8.40 (1H, s), 12.50 (1H, s). ^{13}C NMR (DMSO-d_6) δ ppm: 8.8, 55.7, 108.8, 112.1, 113.6, 122.9, 126.8, 149.6, 151.7, 152.2, 152.7, 153.8. IR (KBr) υ (cm^{-1}): 3254, 2842, 1696, 1609, 1577, 1513, 1271, 1025, 881, 790. MS (ESI) *m/z* (%): 307 (M$^+$, 100), 291 (67), 100 (3). Calcd analysis for $C_{13}H_{14}N_4O_5$: C: 51.0; H: 4.6; N: 18.3. Found: C: 50.8; H: 4.4; N: 18.2.

4.6.1.12. *(E)*-*N*′-(Benzo[*d*][1,3]dioxol-5-yl-methylidene)-3-methylfuroxan-4-carbohydrazide (39). White solid (53%); mp: 197.5–202.8 °C. ^{1}H NMR (acetone-d_6) δ ppm: 2.11 (1H, s), 2.39 (3H, s), 6.94 (1H, d, J = 8.0), 7.22 (1H, dd, J_1 = 8.0, J_2 = 1.3), 7.40 (1H, d, J = 1.3), 8.51 (1H, s), 11.29 (1H, s). ^{13}C NMR (acetone-d_6) δ ppm: 8.13, 102.3, 105.8, 108.6, 112.9, 124.8, 129.0, 149.0, 150.4, 150.6, 151.8, 153.9. IR (KBr) υ (cm^{-1}): 3094, 1713, 1625, 1564, 1269, 1142, 1115, 1057, 928, 1034, 849, 803. MS (EI) *m/z* (%): 290 (M$^+$ 68), 191 (43), 147 (100), 134 (28), 76 (21), 67 (24). Calcd analysis for $C_{12}H_{10}N_4O_5$: C: 49.7; H: 3.5; N: 19.3. Found: C: 49.5; H: 3.1; N: 19.0.

4.6.1.13. *(E)*-*N* ′-(3-Hydroxy-4-methoxyphenylmethylidene)-3-methylfuroxan-4-carbohydrazide (40). Yellow solid (43%); mp: 165.3–168.7 °C. ^{1}H NMR (DMSO-d_6) δ ppm: 2.30 (3H, s), 3.84 (3H, s), 6.80 (1H, d, J = 8.0), 7.10 (1H, d, J = 8.0), 7.32 (1H, s), 8.40 (1H, s), 9.62 (1H, s), 12.36 (1H, s). ^{13}C NMR (DMSO-d_6) δ ppm: 8.9, 56.0, 109.6, 113.6, 115.9, 123.1, 125.2, 148.5, 152.7, 153.7. IR (KBr) υ (cm^{-1}): 3500, 3243, 2830, 1677, 1607, 1592, 1522, 1268, 1036, 883, 849. MS (ESI) *m/z* (%): 293 (M$^{+\cdot}$+H, 25), 277 (6). Calcd analysis for $C_{12}H_{12}N_4O_5$: C: 49.3; H: 4.1; N: 19.2. Found: C: 49.0; H: 4.1; N: 19.0.

4.6.1.14. *(E)*-*N* ′-(4-Hydroxy-3-methoxyphenylmethylidene)-3-methylfuroxan-4-carbohydrazide (41). White solid (55%); mp: 203.0–205.3 °C. ^{1}H NMR (DMSO-d_6) δ ppm: 2.30 (3H, s), 3.82 (3H, s), 6.99 (1H, d, J = 8.0), 7.07 (1H, d, J = 8.0), 7.28 (1H, s), 8.37 (1H, s), 9.39 (1H, s), 12.42 (1H, s). ^{13}C NMR (DMSO-d_6) δ ppm: 8.9, 56.0, 112.3, 112.8, 113.7, 121.4, 126.9, 147.4, 150.8, 151.1, 152.2, 153.8. IR (KBr) υ (cm^{-1}): 3498, 3205, 2850, 1681, 1615, 1576, 1511, 1277, 1029, 882, 779. MS (ESI) *m/z* (%): 293 (M$^{+\cdot}$+H,

58), 277 (47), 100 (4). Calcd analysis for $C_{12}H_{12}N_4O_5$: C: 49.3; H: 4.1; N: 19.2. Found: C: 49.2; H: 3.9; N: 18.9.

4.6.1.15. *(E)-N′*-(4-Carboxyphenylmethylidene)-3-methylfuroxan-4-carbohydrazide (42). Light–yellow solid (98%); mp: 224.8 °C (d). ^{1}H NMR (DMSO-d_6) δ ppm: 2.30 (3H, s), 7.86 (2H, d, J = 8.1), 8.00 (2H, d, J = 8.1), 8.59 (1H, s), 10.11 (1H, s), 12.76 (1H, s). ^{13}C NMR (DMSO-d_6) δ ppm: 8.9, 113.7, 127.9, 130.4, 132.7, 138.2, 149,.8, 152.0, 154.0, 194.0. IR (KBr) υ (cm^{-1}): 3456, 1683, 1612, 1564, 1289, 1039, 902, 842. MS (EI) *m/z* (%): 290 (M$^+$ 13), 191 (47), 148 (46), 67 (100). Calcd analysis for $C_{12}H_{10}N_4O_5$: C: 49.7; H: 3.5; N: 19.3. Found: C: 49.5; H: 3.3; N: 19.5.

4.6.1.16. *(E)*-3-Methyl-*N′*-(4-trifluoromethylphenylmethylidene)furoxan-4-carbohydrazide (43). White solid (52%); mp: 95.0–97.0 °C. ^{1}H NMR (DMSO-d_6) δ ppm: 2.32 (s, 3H), 7.83 (d, 2H J = 8.0), 7.97 (d, 2H J = 8.0), 8.62 (s, 1H), 12.75 (s, 1H). ^{13}C NMR (DMSO-d_6) δ ppm: 8.0, 113.6, 123.1, 126.3, 128.2, 130.9, 138.1, 149.0, 152.0, 154.3. IR (KBr) υ (cm^{-1}): 3405, 3171, 1683, 1622, 1324, 1259. MS (EI) *m/z* (%): 314 (M$^+$ 15), 215 (48), 172 (33), 145 (42), 67 (100). Calcd analysis for $C_{12}H_9F_3N_4O_3$: C: 45.9; H: 2.9; N: 17.8. Found: C: 45.7; H: 2.7; N: 17.5.

4.7. 4-Phenylfuroxan-3-carbohydrazide (VI)[44]

To a solution of (**V**) (74 mg, 0.38 mmol) in dry THF (5 mL), carbonyldiimidazole (68 mg, 0.42 mmol) and the mixture was stirred for 1 h at room temperature. Subsequently, it was slowly added $NH_2NH_2{\cdot}H_2O$ (70%, 0.012 mL) in dry Et_2O (0.5 mL) and the mixture was stirred for 24 h at room temperature. The solvent was evaporated in vacuo and the residue was treated with EtOAc (30 mL) and washed with saturated aqueous solution of Na_2HCO_3. The organic phase was dried with anhydrous Na_2SO_4 and evaporated in vacuo. The product **(VI)**, as a light brown oil (75 mg, 90%), was used without purification in the next reaction.

4.7.1. *(E)-N′*-(4-Carboxyphenylmethylidene)-4-phenylfuroxan-3-carbohydrazide (44)

To a solution of (**VI**) (103 mg, 0.47 mmol) in anhydrous EtOH (2 mL), at 0 °C, was added *p*-formylbenzoic acid (63 mg, 0.42 mmol) and a drop of glacial AcOH. The mixture was stirred for 72 h at room temperature. The solid precipitated was filtered and washed with cold EtOH. Yellow solid (16 mg, 9%); mp: 287.0–289.3 °C. ^{1}H NMR (DMSO-d_6) δ ppm: 7.56 (1H, t, J = 8.0), 7.64 (2H, t, J = 8.0), 7.96 (2H, d, J = 8.0), 7.98 (2H, d, J = 8.0), 8.10 (2H, d, J = 8.0), 8.42 (1H, s), 11.3 (1H, s). ^{13}C NMR (DMSO-d_6) δ ppm: 127.3, 127.4, 128.4, 129.7, 132.1, 132.6, 138.2, 147.9, 165.8. IR (KBr) υ (cm^{-1}): 3075, 2893, 1680, 1634, 1549, 1256, 1076, 865, 776. MS (EI) *m/z* (%): 306 (M$^+$-NO$_2$, 2), 289 (5), 273 (5), 247 (3), 191 (2), 121 (29), 105 (100), 94 (9), 77 (43), 69 (15). Calcd analysis for $C_{17}H_{12}N_4O_5$: C: 58.0; H: 3.4; N: 15.9. Found: C: 57.9; H: 3.1; N: 15.7.

4.8. Biology

4.8.1. NF-κB pathway inhibition assay and IL-8 production

A- *HT-29-NF-κB-hrGFP cells cytotoxicity assay*: HT-29-NF-κB-hrGFP cells (0.5×10^6/mL) were seeded in a 96 well plate in 200 μL fresh culture milieu DMEM (10% fetal bovine serum [FBS], 1% penicillin–streptomycin) and incubated for 24 h at 37 °C and 5% CO_2. The culture milieu was removed and the NAHs, dissolved in DMSO (lower than 0.5%, v/v, in the final volume of DMEM), were added at the desired final concentrations diluted in fresh DMEM (200 μL final volume) (12.5, 25, 50, 100, 200, 400 μM) and the cells were further incubated for 24 h at 37 °C, 5% CO_2. Afterwards, the culture supernatant was removed and cell viability was assessed by measuring the mitochondrial-dependent reduction of 3-(4,5-dimethylthiazol-2yl)-2,5-diphenyltetrazolium bromide (MTT, Sigma) to formazan. For that a solution of MTT, in sterile PBS 0.2% glucose, was added to the cells and incubated for 2 h at 37 °C and 5% CO_2. The supernatant was removed and 180 μL of DMSO and 20 μL MTT buffer (0.1 M glycine, 0.1 M NaCl, 0.5 mM EDTA) was added to each well. Measurements were performed at 560 nm in a spectrophotometer plate reader. B- *NF-kB pathway inhibition assay*: Human intestinal epithelial cells (HT-29, ATCC) were transfected with pNF-κB-hrGFP plasmid (Stratagene) using LipofectAmine 2000 (Invitrogen) and selected with hygromycin (Sigma). After two weeks, cells were stimulated during 24 h with a pro-inflammatory cocktail (25 ng/mL TNF-α, 1.25 ng/mL IL1-B and 3.75 ng/mL IFN-γ) and GFP positive cells were sorted employing a MoFlo instrument (Dako). The responsiveness of the cells towards different concentrations of TNF-α (25–0.2 ng/mL) was tested, the clone showing the best performance was selected for anti-inflammatory screening assays and was named HT-29-NF-κB-hrGFP. HT-29-NF-κB-hrGFP cells (0.5×10^6/mL) were seeded in a 96 well plate in 200 μL fresh DMEM supplemented milieu and were incubated for 24 h at 37 °C, 5% CO_2. Culture milieu was removed and the NAHs, dissolved in DMSO (lower than 0.5%, v/v, in the final volume of DMEM), were added to the cells at the maximum non-cytotoxic concentration diluted in supplemented DMEM milieu (200 μL final volume) and the plate was incubated for 2 h at 37 °C, 5% CO_2. A solution of TNF-α (3 ng/mL final concentration, diluted in complete DMEM) was added and further incubated 18–24 h at 37 °C, 5% CO_2. Three controls were included: 1) Cells treated only with TNF-α but without NAH; 2) Cells treated only with NAH; 3) Cells treated with different Thalidomide concentrations and TNF-α. Supernatants were taken, clarified by centrifugation and stored at −80 °C for further IL-8 determination. Cells were detached by adding 50 μL of trypsin (0.5 g/L trypsin and 0.2 g/L EDTA.4Na, Sigma) to each well, incubated for 5 min at 37 °C, and the trypsin was neutralized by adding 150 μL of complete DMEM milieu. Cell suspensions were transferred into cytometer tubes with PBS (150 μL) and propidium iodide (3 μL of a stock solution of 200 μg/mL). Acquisition and analysis were performed using a CyAn™ ADP (DAKO) flow cytometer and Summit 4.3 software. For each condition, 5000 counts were collected, gated on FSC vs SSC dot plot. Only living cells (cells that excluded propidium iodide) were considered for results comparison and the percentage of GFP positive were normalized against the percentage of GFP cells obtained with the TNF-α control. C- *IL-8 quantitation*: the levels of the proinflammatory cytokine IL-8 was assessed in the cell culture supernatant by flow cytometry using Human Simplex Kit (Bender Medsystems, Austria) and 500 events were collected according to manufacturer recommendations. For results calculation BMS FlowCytomix Software version 2.2.1 was used.

4.8.2. Murine macrophages cytotoxicity

J774 murine macrophage-like cells (ATCC, USA) were maintained in DMEM containing 4 mM L-glutamine, and supplemented with 10% heat-inactivated FBS and 1% penicillin–streptomicin. J774 cells were seeded (1×10^5 cells/well) in 96-well microplates with 100 μL of DMEM supplemented milieu. Cells were allowed to growth for 48 h in a humidified 5% CO_2/95% air atmosphere at 37 °C and, then, exposed to NAHs (25–400 μM) for 48 h. MTT in sterile PBS (0.2% glucose) was added to cells to a final concentration of 0.1 mg/mL and cells were incubated at 37 °C for 3 h. After removing the media, formazan crystals were dissolved in DMSO (180 μL) and MTT buffer (0.1 M glycine, 0.1 M NaCl, 0.5 mM EDTA, 10.5 pH) (20 μL) and the absorbance at 560 nm was read using a microplate spectrophotometer. Results were expressed as IC_{50} (compound concentration that reduced 50% control absorbance

at 560 nm). Every IC_{50} was the average of at least three determinations.

4.8.3. Analgesic activity determinations

Animal studies were approved by the Local Institutional Animal Care and Research Advisory committee. *Acetic acid-induced abdominal constriction assay:* The abdominal constriction assay induced by acetic acid (0.6%; 0.1 mL/10 g) was performed using albino mice of both sexes (18–23 g). Compounds were administered orally (100 μmol/kg) as a suspension in 5% arabic gum in saline solution (vehicle). Dipyrone and indomethacin (100 μmol/kg) were used as standard drug under the same conditions. Acetic acid solution was administered intraperitoneally 1 h after administration of NAHs (**15**, **17**, **20**, **24**, **28**, **31–33**, **36**, **38**, and **42**). Ten minutes following intraperitoneally acetic acid injection the number of constriction per animal was recorded for 20 min. Control animals received an equal volume of vehicle. Analgesic activity was expressed as percentage of inhibition of constrictions when compared with the vehicle control group. Results were expressed as the mean ± SEM of n animals per group. The data were statistically analyzed by the Student *t*-test. *Hot-plate test (hyperalgesia):*[57] Wistar rats of both sexes (150–200 g) were used. The NAHs (**15**, **17**, **24**, and **31**) were administered orally (100 μmol/kg) as a suspension in 5% arabic gum in saline solution (vehicle). Control animals received an equal volume of vehicle. One hour later, the animals were injected with either 0.1 mL of 1% carrageenan solution in saline (1 mg/paw) or sterile saline (NaCl 0.9%), into the subplantar surface of the hind paws respectively. The thermal hyperalgesia was determined using the modified hot-plate test. Rats were placed individually on a hot plate with the temperature adjusted to 51 ± 0.1 °C. The latency of the withdrawal response of the left hind paw was determined at 0, 30, 60, 120, 180, and 240 min post-challenge. The time of maximum permanence permitted on the hot surface was 20 s. Hyperalgesia to heat was defined as a decrease in withdrawal latency and calculated as follows: δ paw withdrawal latency (s) = (left paw withdrawal latency in time 0) − (left paw withdrawal latency in other times). The data were statistically analyzed by the Student *t*-test.

4.8.4. Anti-inflammatory activity determinations

Thirty albino rats of both sexes (150–200 g) were used in this protocol. NAHs (**15**, **17**, **20**, **24**, **28**, **31–33**, **36**, **38**, and **42**) were administered in the dose of choice as a suspension in 1% tween 80 in saline (vehicle). Control animals received equal volume of the vehicle. One hour after, the animals were then injected with either 0.1 mL of 1% carrageenan solution in saline (0.1 mg/paw) or sterile saline (NaCl 0.9%), into the subplantar surface of one of the hind paws, respectively. The paw volumes were measured temporally (for NAHs **15**, **17**, and **31**) and at 3 h after the subplantar injection using a glass plethysmometer coupled to a peristaltic pump. The edema was calculated as the difference of volume between the carrageenan and saline-treated paw. Anti-inflammatory activity was expressed as percentage of inhibition of the edema when compared with vehicle control group. The data were statistically analyzed by the Student *t*-test.

4.8.5. Lipoxygenase inhibition assay

The inhibition of soybean lipoxygenase-15 was initially determined with 50 μM of the respective NAHs (**13–15**, **17**, **18**, **20**, **22–25**, **28**, **31–34**, **36–38**, and **40–44**) according to the manufacturer's instructions (Lipoxygenase Inhibitor Screening Assay Kit—Cayman Chemicals Cat. N° 760700) using araquidonic acid as substrate and H_2O_2 (90 mL of Tris–HCl 0.1 M, pH 7.4, and 10 mL of H_2O_2 420 mM) as lipoxygenated agent. For NAH **42** IC_{50} was determined varying the studied concentrations (10–100 μM). Quercetin (4 μM) was used as positive control. Results were calculated as the means of duplicate determinations. The data were statistically analyzed by the Student *t*-test.

4.8.6. COXs inhibition assay

The inhibition of isolated ovine COX-1 and human recombinant COX-2 was determined with 10 and 50 μM of the respective NAHs (**17**, **24**, and **31**) by ELISA according to the manufacturer's instructions ('COX inhibitor screening assay', Cayman Chemical Cat. N° 560131). Indomethacin (0.1 μM for COX-1 and 6 μM for COX-2) was used as positive control. Results were calculated as mean of duplicate determinations. The data were analyzed by the Student *t*-test.

4.8.7. Nitric oxide release determinations

An Apollo 4000 electrode—Free radical analyzer Instrumental (World Precision Instruments) an ISO-NO membrane and an ISO-NOP sensor were used to measure NO release. The compounds (**15**, **17**, **18**, **20**, **24**, **41**, **42**, and **44**) dissolved in DMSO, were incorporated to the work buffer, Tris–HCl 0.1 M, DTPA 0.1 mM, pH 7.4 or 8.3. Cysteine (300 or 100 μM) was added and the NO production was registered for 20 min at 25 or 37 °C.

4.8.8. Mutagenicity assay

The method of direct incubation in plate was performed. Culture of *S. typhimurium* TA98 strain in the agar minimum glucose milieu (AMG)—agar solution, Vogel Bonner E(VB) 50×, and 40% glucose solution—was used. First, the direct toxicity of the compounds under study against *S. typhimurium* TA98 strain was assayed. DMSO solutions of **17**, **24**, **31**, and **42** at different doses (starting at the highest doses without toxic effects, 250.0 or 350.0 μg/plate) were assayed in triplicate. Positive controls of 4-nitro-*o*-phenylendiamine (20.0 μg/plate, in the run without S9 activation) and 2-aminofluorene (10.0 μg/plate, in the cases of S9 activation) and negative control of DMSO were run in parallel. The influence of metabolic activation was tested by adding 500 μL of S9 fraction of mouse liver treated with Aroclor, obtained from Moltox, Inc. (Annapolis, MD, USA). The revertant number was counted manually. The sample was considered mutagenic when the number of revertant colonies was at least double that of the negative control for at least two consecutive dose levels.

Acknowledgements

We thank PEDECIBA-ANII for scholarship to P.H., M.C., L.C., and CNPq-PROSUL network for fellowships to P.H. E.J.B., A.L.P.M. and L.M.L. thanks CNPq (BR) for fellowships. We thank INCT-INOFAR (CNPq CNPq 573.564/2008-6 and FAPERJ E-26/170.020/2008) for partial financial support.

Supplementary data

Supplementary data (spectroscopy characterization, and biological data (eight pages)) associated with this article can be found, in the online version, at doi:10.1016/j.bmc.2012.01.034.

References and notes

1. Nathan, C. *Nature* **2002**, *420*, 846.
2. Williams, M.; Kowaluk, E. A.; Arneric, S. P. *J. Med. Chem.* **1999**, *42*, 1481.
3. Smith, W. L.; Meade, E. A.; DeWitt, D. L. *Ann. N.Y. Acad. Sci.* **1994**, *714*, 136.
4. Vane, J.; Bakhle, Y. S.; Botting, R. M. *Ann. Rev. Pharmacol. Toxicol.* **1998**, *38*, 97.
5. Whittle, B. J. R.; Higgs, G. A.; Eakins, K. E.; Moncada, S.; Vane, J. R. *Nature* **1980**, *284*, 271.
6. Xie, W.; Robertson, D. L.; Simmons, D. L. *Drug Dev. Res.* **1992**, *25*, 249.
7. Penning, T. D.; Talley, J. J.; Bertenshaw, S. R.; Carter, J. S.; Collins, P. W. *J. Med. Chem.* **1997**, *40*, 1347.
8. Talley, J. J.; Brown, D. L.; Carter, J. S.; Graneto, M. J.; Koboldt, C. M.; Masferrer, J. L.; Perkins, W. E.; Rogers, R. S.; Shaffer, A. F.; Zhang, Y. Y.; Zweifel, B. S.; Seibert, K. *J. Med. Chem.* **2000**, *43*, 775.

9. Brophy, J. M. *Curr. Opin. Gastroenterol.* **2007**, *23*, 617.
10. Mukherjee, D.; Nissen, S. E.; Topol, E. J. *J. Am. Med. Assoc.* **2001**, *286*, 954.
11. Allison, M. C.; Howatson, A. G.; Torrance, C. J.; Lee, F. D.; Russel, R. I. G. N. *Engl. J. Med.* **1992**, *327*, 749.
12. Khannaa, I. S.; Weier, R. M.; Collins, P. W.; Miyashiro, J. M.; Koboldt, C. M.; Veenhuizen, A. W.; Currie, J. L.; Seibert, K.; Isakson, P. C. *J. Med. Chem.* **1997**, *40*, 1619.
13. Boehm, J. C.; Smietana, J. M.; Sorenson, M. E.; Garigipati, R. S.; Gallagher, T. F.; Sheldrake, P. L.; Bradbeer, J.; Badger, A. M.; Laydon, J. T.; Lee, J. C.; Hillegass, L. M.; Griswold, D. E.; Breton, J. J.; Chabot-Fletcher, M. C.; Adams, J. L. *J. Med. Chem.* **1996**, *39*, 3929.
14. Li, J. J.; Anderson, G. D.; Burton, E. G.; Cogburn, J. N.; Collins, J. T.; Garland, D. J.; Gregory, S. A.; Huang, H. C.; Isakson, P. C.; Koboldt, C. M.; Logusch, E. W.; Norton, M. B.; Perkins, W. E.; Reinhart, E. J.; Seibert, K.; Veenhuizen, A. W.; Zhang, Y.; Reitz, D. B. *J. Med. Chem.* **1995**, *38*, 4570.
15. Lima, P. C.; Lima, L. M.; Silva, K. C. M.; Léda, P. H. O.; Miranda, A. L. P.; Fraga, C. A. M.; Barreiro, E. J. *Eur. J. Med. Chem.* **2000**, *35*, 187.
16. Bezerra-Neto, H. J. C.; Lacerda, D. I.; Miranda, A. L. P.; Alves, H. M.; Barreiro, E. J.; Fraga, C. A. M. *Bioorg. Med. Chem.* **2006**, *14*, 7924.
17. Duarte, C. D.; Tributino, J. L. M.; Lacerda, D. I.; Martins, M. V.; Alexandre-Moreira, M. S.; Dutra, F.; Bechara, E. J. H.; De-Paula, F. S.; Goulart, M. O. F.; Ferreira, J.; Calixto, J. B.; Nunes, M. P.; Bertho, A. L.; Miranda, A. L. P.; Barreiro, E. J.; Fraga, C. A. M. *Bioorg. Med. Chem.* **2007**, *15*, 2421.
18. Cunha, A. C.; Figueiredo, J. M.; Tributino, J. L. M.; Miranda, A. L. P.; Castro, H. C.; Zingali, R. B.; Fraga, C. A. M.; de Souza, M. C. B. V.; Ferreira, V. F.; Barreiro, E. J. *Bioorg. Med. Chem.* **2003**, *11*, 2051.
19. Silva, G. A.; Costa, L. M. M.; Brito, F. C. F.; Miranda, A. L. P.; Barreiro, E. J.; Fraga, C. A. M. *Bioorg. Med. Chem.* **2004**, *12*, 3149.
20. Lima, L. M.; Frattani, F. S.; dos Santos, J. L.; Castro, H. C.; Fraga, C. A. M.; Zingali, R. B.; Barreiro, E. J. *Eur. J. Med. Chem.* **2008**, *43*, 348.
21. Tributino, J. L. M.; Duarte, C. D.; Corrêa, R. S.; Dorigetto, A. C.; Ellena, J.; Romeiro, N. C.; Castro, N. G.; Miranda, A. L. P.; Barreiro, E. J.; Fraga, C. A. M. *Biorg. Med. Chem.* **2009**, *17*, 1125.
22. Gonzalez-Serratos, H.; Chang, R.; Pereira, E. F.; Castro, N. G.; Aracava, Y.; Melo, P. A.; Lima, P. C.; Fraga, C. A. M.; Barreiro, E. J.; Albuquerque, E. X. *J. Pharmacol. Exp. Ther.* **2001**, *299*, 558.
23. Silva, A. G.; Zapata-Sudo, G.; Kummerle, A. E.; Fraga, C. A. M.; Barreiro, E. J.; Sudo, R. T. *Bioorg. Med. Chem.* **2005**, *13*, 3431.
24. Barreiro, E. J.; Fraga, C. A. M.; Miranda, A. L. P.; Rodrigues, C. R. *Quím. Nova* **2002**, *25*, 129.
25. Mahy, J. P.; Gaspard, S.; Mansuy, D. *Biochemistry* **1993**, *32*, 4014.
26. Maia, R. C.; Silva, L. L.; Mazzeu, E. F.; Fumian, M. M.; de Rezende, C. M.; Doriguetto, A. C.; Corrêa, R. S.; Miranda, A. L. P.; Barreiro, E. J.; Manssour Fraga, C. A. *Bioorg. Med. Chem.* **2009**, *17*, 6517.
27. Ribeiro, I. G.; da Silva, K. C. M.; Parrini, S. C.; de Miranda, A. L. P.; Fraga, C. A. M.; Barreiro, E. J. *Eur. J. Med. Chem.* **1998**, *33*, 225.
28. Figueiredo, J. M.; Câmara, C. A.; Amarante, E. G.; Miranda, A. L. P.; Santos, F. M.; Rodrigues, C. R.; Fraga, C. A. M.; Barreiro, E. J. *Bioorg. Med. Chem.* **2000**, *8*, 2243.
29. Fraga, C. A.; Barreiro, E. J. *Curr. Med. Chem.* **2006**, *13*, 167.
30. Barja-Fidalgo, C.; Fierro, I. M.; Brando Lima, A. C.; Teixeira Da Silva, E.; De Amorim Câmara, C.; Barreiro, E. J. *J. Pharm. Pharmacol.* **1999**, *51*, 703.
31. Pontiki, E.; Hadjipavlou-Litina, D. *Med. Chem.* **2007**, *3*, 175.
32. Turnbull, C. M.; Marcarino, P.; Sheldrake, T. A.; Lazzarato, L.; Cena, C.; Fruttero, R.; Gasco, A.; Fox, S.; Megson, I. L.; Rossi, A. G. *J. Inflamm.* **2008**, *5*, 12.
33. Velázquez, C.; Praveen Rao, P. N.; McDonald, R.; Knaus, E. E. *Bioorg. Med. Chem.* **2005**, *13*, 2749.
34. Fang, L.; Zhang, Y.; Lehmann, J.; Wang, Y.; Ji, H.; Ding, D. *Bioorg. Med. Chem. Lett.* **2007**, *17*, 1062.
35. Chalimoniuk, M.; Głowacka, J.; Zabielna, A.; Eckert, A.; Strosznajder, J. B. *Neurochem. Int.* **2006**, *48*, 1.
36. Chalimoniuk, M.; Stolecka, A.; Cakała, M.; Hauptmann, S.; Schulz, K.; Lipka, U.; Leuner, K.; Eckert, A.; Muller, W. E.; Strosznajder, J. B. *Acta Biochim. Polon.* **2007**, *54*, 611.
37. Barriga, G.; Olea-Azar, C.; Norambuena, E.; Castro, A.; Porcal, W.; Gerpe, A.; González, M.; Cerecetto, H. *Bioorg. Med. Chem.* **2010**, *18*, 795.
38. Isomoto, H.; Saenko, V. A.; Kanazawa, Y.; Nishi, Y.; Ohtsuru, A.; Inoue, K.; Akazawa, Y.; Takeshima, F.; Omagari, K.; Miyazaki, M.; Mizuta, Y.; Murata, I.; Yamashita, S.; Kohno, S. *Am. J. Gastroenterol.* **2010**, *99*, 589.
39. Barreiro, E. J.; Costa, P. R. R.; Coelho, F. A. S.; de Farias, F. M. C. *J. Chem. Res.* **1985**, 2301.
40. Dias, L. R. S.; Alvim, M. J. F.; Freitas, A. C. C.; Barreiro, E. J.; Miranda, A. L. P. *Pharm. Acta Helv.* **1994**, *69*, 163.
41. Yamada, S.; Morizono, D.; Yamamoto, K. *Tetrahedron Lett.* **1992**, *33*, 4329.
42. Lai, G.; Anderson, W. K. *Synth. Commun.* **1997**, *27*, 1281.
43. de Barros, F. R. C.; Leite, L. F. C. C.; dos Santos Filho, J. M.; de Lima, J. G. *Anais. Assoc. Bras. Quim.* **2001**, *50*, 162.
44. Koufaki, M.; Calogeropoulou, T.; Detsi, A.; Roditis, A.; Kourounakis, A. P.; Papazafiri, P.; Tsiakitzis, K.; Gaitanaki, C.; Beis, I.; Kourounakis, P. N. *J. Med. Chem.* **2001**, *44*, 4300.
45. a Karabatsos, G. J.; Graham, J. D.; Vane, F. M. *J. Am. Chem. Soc.* **1962**, *84*, 753; b Karabatsos, G. J.; Shapiro, B. L.; Vane, F. M.; Fleming, J. S.; Ratka, J. S. *J. Am. Chem. Soc.* **1963**, *85*, 2784; c Karabatsos, G. J.; Taller, R. A. *J. Am. Chem. Soc.* **1963**, *85*, 3624.
46. Sommer, M.; Kress, M. *Neurosci. Lett.* **2004**, *361*, 184.
47. a Gaffney, B. J. *Annu. Rev. Biophys. Biomol. Struct.* **1996**, *25*, 431; b Mascayano, C.; Núñez, G.; Acevedo, W.; Rezende, M. C. *J. Mol. Model.* **2010**, *16*, 1039.
48. Blobaum, A. L.; Marnett, L. J. *J. Med. Chem.* **2007**, *50*, 1425.
49. López, G. V.; Batthyány, C.; Blanco, F.; Botti, H.; Trostchansky, A.; Migliaro, E.; Radi, R.; González, M.; Cerecetto, H.; Rubbo, H. *Bioorg. Med. Chem.* **2005**, *13*, 5787.
50. Maron, D. M.; Ames, B. N. *Mutat. Res.* **1983**, *113*, 173.
51. Chu, K. C.; Patel, K. M.; Lin, A. H.; Tarone, R. E.; Linhart, M. S.; Dunkel, V. C. *Mutat. Res.* **1981**, *85*, 119.
52. Ye, Q.; Chen, B.; Tong, Z.; Nakamura, S.; Sarria, R.; Costabel, U.; Guzman, J. *Eur. Respir. J.* **2006**, *28*, 824.
53. a Sullivan, R. W.; Bigam, C. G.; Erdman, P. E.; Palanki, M. S. S.; Anderson, D. W.; Goldman, M. E.; Ransone, L. J.; Suto, M. J. *J. Med. Chem.* **1998**, *41*, 413; b Zhang, H.-C.; Derian, C. K.; McComsey, D. F.; White, K. B.; Ye, H.; Hecker, L. R.; Li, J.; Addo, M. F.; Croll, D.; Eckardt, A. J.; Smith, C. E.; Li, Q.; Cheung, W.-M.; Conway, B. R.; Emanuel, S.; Demarest, K. T.; Andrade-Gordon, P.; Damiano, B. P.; Maryanoff, B. E. *J. Med. Chem.* **2005**, *48*, 1725; c Yasui, T.; Yamada, M.; Uemura, H.; Ueno, S.; Numata, S.; Ohmori, T.; Tsuchiya, N.; Noguchi, M.; Yuzurihara, M.; Kase, Y.; Irahara, M. *Maturitas* **2009**, *62*, 146.
54. Fruttero, R.; Ferrarotti, B.; Serafino, A.; Di Stilo, A.; Gasco, A. *J. Heterocycl. Chem.* **1989**, *26*, 1345.
55. Porcal, W.; Merlino, A.; Boiani, M.; Gerpe, A.; González, M.; Cerecetto, H. *Org. Process Res. Dev.* **2008**, *12*, 156.
56. Gasco, A. M.; Fruttero, R.; Sorba, G.; Gasco, A. *Liebigs Ann. Chem.* **1991**, 1211.
57. Lavich, T. R.; Cordeiro, R. S. B.; Silva, P. M. R.; Martins, M. A. *Braz. J. Med. Biol. Res.* **2005**, *38*, 445.